CONTROLLED RELEASE OF ETORICOXIB FROM POLY(ESTER UREA) FILMS FOR POST-OPERATIVE PAIN MANAGEMENT

A Thesis

Presented to

The Graduate Faculty of The University of Akron

In Partial Fulfillment

of the Requirements for the Degree

Master of Polymer Science

Natasha Brigham

August, 2019

CONTROLLED RELEASE OF ETORICOXIB FROM

POLY(ESTER UREA) FILMS FOR

POST-OPERATIVE PAIN MANAGEMENT

Natasha Brigham

Thesis

Approved:	Accepted:
_____	_____
Advisor Dr. Matthew Becker	Dean of the College Dr. Ali Dhinojwala
_____	_____
Faculty Reader Dr. Andrey Dobrynin	Dean of the Graduate School Dr. Chand Midha
_____	_____
Department Chair Dr. Tianbo Liu	Date

ABSTRACT

Adequate post-operative pain management has been proven to enhance the healing and recovery of patients following most major procedures.[1] However, it remains significantly under managed and is a serious unmet need in the medical field. The mainstay of post-operative pain management is the prescription of oral opioids, which, although effective, have many pitfalls. Most notably, opioids prescriptions are currently based on a "one-size-fits-all" model, providing an imbalance of doses given to patients and leaving the medication at the risk for misuse and abuse.

Opioids are still in practice today ultimately due to a lack of a better solution. Herein, we propose a drug-loaded polymer film to control post-operative pain. Poly(ester urea)s were used to load drugs into solvent cast blade-coated films and tested for drug release of non-opioids agents. Specifically, etoricoxib, a selective cyclooxygenase isoform 2 (COX-2) was used to monitor the efficacy of delivery from these films both *in vitro* and in a rat model. To obtain different release profiles, film thickness, drug-load, and polymer composition was analyzed in order to get desired profile for analgesic release. The polymer analogs that were implemented for this study are copolymers, 10%, 20% and 30% 1-PHE-6 P(1-VAL-8), and homopolymers, P(1-VAL-8), P(1-VAL-10), and P(1-VAL-12). Moreover, a multi-modal analgesia model with bupivacaine (a local anesthetic) has been sought out to show the versatility of this device. The goal of this study was to study a controlled release system that will produce little to no inflammation

while providing pain relief for 3-5 days following a surgical procedure. Ultimately, this device's intended purpose is to replace or minimize the need for prescription opioids. We hypothesize that by tuning the multiple factors available with PEUs that a variety of drug release profiles can be obtained to fit a number of different applications (i.e. acute to chronic pain).

Keywords: poly(ester urea), post-operative pain management, etoricoxib, bupivacaine, controlled drug release

ACKNOWLEDGEMENTS

I would first and foremost like to give a big thank-you to my advisor, Dr. Matthew Becker, who has given me extensive support throughout this entire process. Without the opportunities he has offered me and without his mentorship, I know that I would not be anywhere near the researcher that I am today. I consider myself very fortunate that he offered me a summer position in his lab before my degree program began. I would like to acknowledge Dr. Andrey Dobrynin for agreeing to be on my committee and being a reader.

I would also like to specifically thank Alexandra Abel and Nathan Dreger for being my mentors. I appreciate all of your help on a professional and academic level, but also your mental support that I gained from our friendship. You both made work productive and so much fun at the same time. Thank you to my entire group for being so inclusive and providing a friendly and collaborative work environment.

Importantly, I would like to thank my colleagues at Merck for allowing me to spend an entire summer under their supervision and allowing me to experience industrial research. This experience was truly invaluable, and I know that I have grown significantly as a researcher because of it.

Lastly, but definitely not least, I would like to thank my family and friends, for being my outlet away from academics and allowing me to get the mental break that I needed every now and again. Without their support, my graduate school career would have been much more stressful. Once again, thank you to everyone that has impacted my life and helped me throughout this journey.

TABLE OF CONTENTS

LIST OF TABLES

Table Page

LIST OF FIGURES

LIST OF SCHEMES

Scheme Page

CHAPTER 1

INTRODUCTION

Approximately 234 million surgeries are performed around the world annually[2], of which postoperative pain is reported in at least 75% of patients following any major procedure.[3] Although a seemingly obvious side effect of any operation, proper pain management following a medical procedure is crucial to enhancement of patient recovery thereafter.[1,4] Moreover, inadequate treatment of pain postoperatively can lead to additional medical and psychological changes that may decrease the patient's quality of life, as well as causing increased medical costs. Despite advancements in current technology, pain management remains a challenge because treatment methods are not a one size fits all solution. Even under identical surgeries, management strategies are highly variable with large deviations required from person to person. This has led to physicians taking an overestimated approach when prescribing pain management drugs where patients can take analgesics "as needed". While in principle this approach is fine, when the quantity and strength of prescribed drug vastly exceeds the amount required to achieve analgesia, the potential for drug abuse becomes prominent.

Despite the movements to address the opioid epidemic, the current methods for patient analgesia following a surgery commonly involve the prescription of opioids in the oral dosage form or pain management, such as intravenous administration, provoking a

prolonged hospital stay. Most strategies in shifting away from opioid use have focused on long-term prescriptions rather than

outpatient prescriptions.[5,6] The number of opioids prescribed perioperatively varies widely between patients and prescribing physicians, but is almost always prescribed in excess. This disproportionally leaves first time opioid users at risk for drug abuse with 1 in 16 opioid-naïve patients becoming long-time users after surgery.[7,8] Considering the risks associated with the current practices, postoperative analgesia alternatives are constantly emerging in new literature, though none have made significant headway yet.[9–14]

CHAPTER II

BACKGROUND

With the ever-changing technology available in medical professions, the goal remains constant: to give patients the best treatment possible. Unfortunately, post-operative pain management still involves very generalized methods for analgesia. However, pain is a very subjective physiological process and therefore, should be treated in a more case-to-case manner. The implementation of biomaterials into controlled release systems is one step in the right direction to accessing tunable devices that can be tailored individually per patient.

The global biomaterials market is currently valued at $84 billion and is excepted to grow exponentially by the year 2025.[15] The growth in the market share can be attributed to the rising occurrence of diseases and orthopedic injuries, in which biomaterials have and will continue to play a pivotal role in the development of implantable structures for support or therapy. Both natural and synthetic materials have been explored for biomedical applications, though synthetic materials are more practical. Synthetic materials can be classified into three different groups: metals, bio-ceramics and polymers. Polymers by far hold the largest market share of the global biomaterials market, displacing the once popular metal materials due to their production methods, low costs, and properties.[16] Moreover,

polymers have found use in a variety of applications such as tissue engineering,[17] plastic surgery,[18] drug delivery devices,[19] and other medical implants.[20,21]

According to the 2019 market report, advanced drug delivery systems are expected to register an increased market share between the years 2019 to 2024, with the current market valued at $280 billion. The main focus behind the new technology will be towards increased drug bioavailability and efficiency of delivery systems. Many different materials have been explored for controlled drug delivery. However, synthetic polymers afford the most synthetic flexibility, cost effectiveness, and versatility when it comes to encapsulation of different drugs and will be the focus of discussion herein.

Drug release from polymer systems can be controlled by diffusion, polymer degradation, solvent swelling or/and responses to external factors depending on both the polymer and drug. Often drug release is dependent on more than one of these factors in tandem with one another. Moreover, due to the synthetic tunability of most polymers, the system can be specifically tuned to fit a specific model based on their degradation mechanisms. In terms of material used, polymers can impact drug release by following either a surface or bulk degradation. Ultimately, this changes how the drug will be release to the surrounding environment.

2.1. Surface Eroding Polymers

In a surface eroding material, degradation occurs from the exterior surface and is usually characteristic of labile bonds that get exposed at the surface, but an overall hydrophobic structure. Surface erosion polymers, when considered for drug delivery, are characteristic of consistent release rates that are proportional to the polymer degradation

(Figure 2.1). A few examples of polymers in this category that have already been utilized for drug release are polyanhydrides and poly(ortho esters).

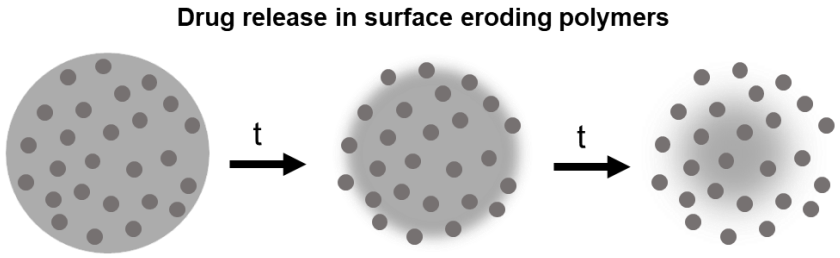

Figure 2.1. Diagram exemplifying a surface eroding polymeric material. These materials degrade in a "layer-by-layer" fashion and release drug accordingly at a zero-order rate.

2.1.1. Polyanhydrides

Much of the work involving polyanhydrides as biomaterials was conducted by Langer and colleagues.[22–25] Unlike many of the polymers used for drug delivery, the labile anhydride bond in the polymer backbone, but overall hydrophobicity make polyanhydrides a surface eroding, and therefore heterogeneously degradable material.[24] This property allows for drug release that is closer to zero order. Water cannot penetrate the bulk of the material until the surface is weakened hydrolytically in a "layer-by-layer" fashion. Polyanhydrides are considered one of the most hydrolytically reactive biomaterials and have the capability to achieve a very high rate of degradation. Moreover, by tuning the hydrophobicity, an array of degradation profiles lasting a week to year are possible.[26,27]

A potential limitation of polyanhydrides for drug release purposes is the reactivity of the polymer with various amines that has been exhibited at high-temperatures. Therefore, the reactivity of the active agent for sustained delivery must be considered prior to introducing it into a polyanhydride matrix. However, polyanhydrides have been

introduced in various fabrications and studied for their ability to release small molecules,[28] proteins,[29–31] bioactive agents to promote bone formation,[31,32] and more popularly, chemotherapeutic drugs.[33–36]

Polyanhydrides were one of the first materials to gain government approval aside from polyesters. Gliadel® Wafer is a polyanhydride material that was approved early on by the FDA for the delivery of BCNU (bis-chloroethylnitrosourea) directly to the brain to treat glioblastoma multiformae.[37] The wafer is comprised of poly[bis(pcarboxyphenoxy) propane: sebacic acid] in a 20:80 molar ratio and 7.7 mg of drug (in a 200 mg wafer). The polymer is shown to degrade quickly, with more than 70% mass gone in three weeks. The byproducts are readily metabolized by bodily functions and the matrix improved patient survival by 20%.

In another product, a polyanhydride copolymer comprising on erucic acid dimer and sebacic acid in a 1:1 weight ratio has been developed for the treatment of osteomyelitis (Septacin™). In this model, controlled release of gentamicin sulfate from the polyanhydride matrix has been exhibited and shown to be impacted by the *in vitro* media.[38] Further studies of this system reveal the ability of it to maintain low levels of systemic exposure while exhibiting efficacy in infection models.[39]

2.1.2. Poly(orthoesters)

Another group of polymers that are surface erodible that have been used in drug delivery are polyorthoesters. Two major types of poly(ortho esters) are available today. Originally, these polymers were prepared by a condensation reaction of 2,2-diethoxytetrahydrofuran and a di-alcohol (Chronomer™ and Alzamer®).[40] This set of

polymers undergo rapid degradation due to the production of γ-butyric acid upon hydrolysis. In more recent work, *Heller et al.* synthesized a new type of poly(ortho ester) with the reaction of 3,9-bis(ethylidene 2,4,8,10-tetraoxaspiro {5,5} undecane) (DETOSU) with various di-alcohols.[41] By synthesizing poly(orthoesters) by this method, no acidic byproduct is produced and, thus, degradation does not proceed in an autocatalytic manner.

Depending on the nature of the diol used in the synthesis, solid polymers or viscous semi-solid materials are obtainable with poly(ortho ester)s, leaving high flexibility in fabrication of drug delivery vehicles. Drug delivery has been exhibited with poly(orthoesters) and appears to follow a predominantly erosion-controlled path.[42] Poly(ortho esters) have been used to delivery small-molecules[43] as well as macromolecules, such as proteins.[44] Moreover, in their lab, *Heller et al*. are working on the development of poly(ortho ester) gels for post-surgical pain management with the controlled delivery of mepivacaine, as outlined in their review.[45]

2.2. Bulk Eroding Polymers

Bulk erosion occurs throughout the entirety of the material. As such, these polymers tend to be more hydrophilic than surface eroding materials, thus allowing for water to penetrate the surface and degrade the material from the bulk (Figure 2.2).

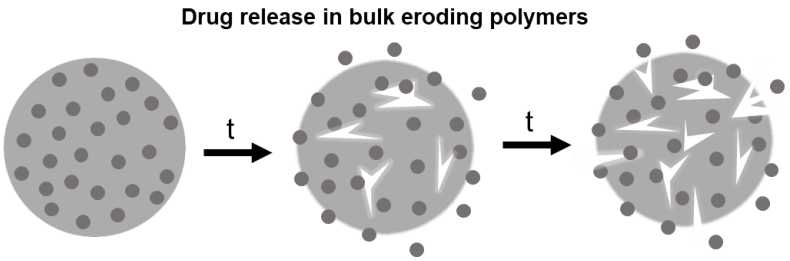

Figure 2.2. An example of a bulk eroding polymeric material. These polymers degrade throughout the entire material, not just at the surface that is exposed to the environment. These polymers usually allow for hydrolytic penetration and degrade due to that.

2.2.1. Poly(ethylene glycol)

Poly(ethylene glycol) (PEG) is one of the most used polymer in the biomedical field in general, and in the relatively more recent developing field of drug delivery. Due to its hydrophilicity, PEG is often used to introduced stealth behavior for drug delivery (PEGylation). The addition of PEG to different hydrophobic polymers allows for formation of micellular or liposomal structures and provides the effective shielding of the encapsulated species from the external environment. Since the discovery of this, PEG has been incorporated into a vast amount of different drug delivery applications that have been outlined in a few different reviews.[46,47] Although there is little research on PEG specific matrices for application in controlled drug delivery, copolymers and other PEGylated products for this purpose have been studied in the literature and will be discussed later on.

2.2.2. Poly(ε-caprolactone)

Poly(ε-caprolactone) (PCL) is an aliphatic polyester that is one of the slower degrading materials used for drug delivery to date. The slow degradation of PCL can be attributed to it's semi-crystalline behavior and hydrophobicity. Under specific environmental conditions, both hydrolytic and enzymatic surface degradation are possible.

Given the length of the degradation time, PCL is more suited for long-acting, implantable devices such as Capronor®, a one-year implantable contraceptive device.[48] Moreover, PCL has a low melting temperature, and exhibits high thermal stability, rendering it useful for processability. PCL has also been combined with a variety of different polymers in order to obtain different mechanical properties and degradation profiles, such as poly(ethylene glycol) (PEG) and poly(lactic acid) (PLA).

PCL-PEG-PCL nanoparticles loaded with lidocaine were developed for dispersion into a gel system for an injectable form of sustained pain management.[49] In this system, the hydrophobic PCL components was utilized as the core to form a micelle-like structure in which the lidocaine was loaded. When injected into a rat, the nanoparticle gel performed superior to control groups by inducing topical transdermal analgesia in more rats. Additionally, PCL was combined with PLA in a triblock copolymer to form a biodegradable thermoplastic elastomer.[50]

2.2.3. Poly(lactic-co-glycolic acid)

Poly(lactic-*co*-glycolic acid) (PLGA) is currently one of the most widely used polymers for controlled drug delivery. Both the copolymer and it's corresponding homopolymers, poly(glycolic acid) (PGA) and poly(lactic acid) (PLA) are biodegradable polymers that were initially studied for their application as surgical sutures in the early 1960's.[51,52] This application sparked their journey into becoming one of the most widely used resorbable biomaterials in the field, and eventually led to their high prevalence in the controlled drug delivery realm. Since then, PLGA is of great use in the biomedical

community due to its aptitude for tunability (crystallinity, hydrolysis rate, molecular weight, hydrophobicity, etc.), biodegradability and high mechanical strength.

PLGA has been used to delivery many molecules from large scale, such as proteins[53] and hormones,[54] to small, such as anti-biotics[55,56] and analgesics.[12,57] By controlling the weight ratio of PLA to PGA, the hydrophilicity of the material can be changed, allowing for an array of molecules (hydrophobic and hydrophilic) to be incorporated into the polymer matrix in a compatible manner.[58] Moreover, this also changes the rate at which water can penetrate the drug delivery device, thus imparting control over the degradation rate and delivery rate. PLGA's byproducts are readily metabolized by the body *via* the tricarboxylic acid cycle, and thus present little to no threat to the normal biological processes and offers a productive environmental characteristic.

A large portion of the work done on PLGA for drug delivery has been in the form of nano- or micro-particles. They have been prepared with various different methods and produced in a vast number of geometries. Current products using PLGA particles include Lupron Depot® (Abbott Laboratories, USA) and Trelstar® (Watson Pharmaceuticals, USA) for sustained release of leuprolide and triptorelin, respectively. Additionally, academic research has unveiled PLGA nanoparticles for delivery of substances to otherwise difficult biological areas (e.g. penetration of muscus linings in the vagina[59] and lungs[60]), and non-encapsulative protein delivery in hydrogels.[61] Work done on PLGA formulations indicate that the material accumulates rapidly in liver, bone marrow, lymph nodes, spleen and peritoneal macrophages and that degradation follows a period of haste followed by a slowing down and the material is then cleared by the lungs.[62] In light of these limitations and to get different material properties and to improve drug delivery, a method

for PLGA copolymerization with other polyesters or biodegradable polymers, such as poly(ethylene glycol) (PEG), has been well established.

In diblocks of PLGA-PEG, micelles can be formed and used in drug delivery to completely surround the encapsulated species. With the PEG layer as a barrier, these release vesicles prevent external or foreign material from interaction and interfering with the encapsulated species, increasing stability and therefore shelf life of the system.[63] Alternatively, triblocks (ABA or BAB) have been developed to form thermogels.[64,65] In this system, the hydrogen bonding between the polymer chains plays a critical role and allows for experimentation of various properties. Release from these triblocks occurs in two phases: (i) drug diffusion in the initial release stage and (ii) erosion of the hydrogel matrix during the later phase. Many different versions of PLGA and its homopolymers have been used to obtain specific drug delivery rates and mechanical properties for various biomedical applications.

Wang et al. were able to demonstrate the effectiveness of using PEG-PLA to form ropivacaine-loaded nanoparticles for post-operative applications.[66] In this model, a 30% burst of drug was observed in 10 hours in vivo, and could provide hyperalgesia to the animal for 3 days following incision. The hydrophilicity of the polymer as well as the small particle size was attributed to these relatively short provided times for analgesia. These results might be able to be altered and release duration lengthened by tuning some of the factors in fabrication, such as hydrophobicity of the polymer.

In a different fabrication, *Tabata et al.* were able to demonstrate the relief of post-surgical pain in rats using a PLGA slow-releasing lidocaine sheet (SRLS).[67] A considerably high amount of lidocaine was loaded into these sheets (30% w/w), providing an efficient

system for delivery of a local anesthetic. *In vitro,* 50% of the lidocaine was released from the film into phosphate buffer solution in 3 days, and 90% in 7 days. These results were similar to those seen in the rat model, with 50% of the drug releasing in 2 days and 5% left in the SRLS after the completion of the study (day 7). By controlling the release of analgesic to the body, the bioavailability is more sustained. In comparison to exposure to free drug, controlled drug delivery was able to provide hypersensitivity for several days, rather than just for a few hours.[67] In light of it's admirable successes, PLGA has been associated with increased risk of inflammatory response due to it's acidic degradation byproducts, causing acidosis to local tissue.[68] Thus, it's application in larger scale biomedical devices has been limited.

2.2.4. Poly(ester urea)

Unlike PLGA, poly(ester urea)s (PEUs) are a novel class of polymers that do not promote inflammatory response due to their degradation.[69] Moreover, the composition of the polymer backbone of PEUs can be altered to obtain an array of different characteristics. PEUs have already exhibited an extensive variety of mechanical properties that have allowed them to be proposed as applications ranging from vascular stents to bone fixture implants.[70,71] By imparting flexibility over the chemical structure of PEUs, different water uptake capability, degrees of hydrogen bonding, and degradation profiles as also possible. Considering all of these useful properties, PEUs have the potential to side step the current issues with PLGA drug delivery devices and prove their worth as a top-tier controlled release system. As a polymer that is new to the field, these materials have yet to be

exhausted of their biomaterial applications and have the potential to make significant headway in the near future.

2.3. Pain Management and Current Treatment Methods

Very little of the work thus far done involving polymers for controlled drug release has included targeting surgical pain management. Despite the continuous advances in pain management research, postoperative pain has been undermanaged for decades. Pain and inflammation is common after many surgical procedures as the body's natural defense mechanism to injury; more than 80% of patients who undergo surgery report experiencing acute pain following the procedure.[3,72] Moreover, less than half of these patients report receiving adequate postoperative analgesia.[72] Prescription opioids remain the backbone to treat post-operative pain regardless of the strong evidence suggesting the dangers involved with them. Other methods of achieving analgesia exist, but the evidence supporting them is disappointing. Therefore, opioids continue to be the mainstay until a more promising solution is proposed.

2.3.1.1. Opioid Therapy

Specifically, more than 80% of patients reported being prescribed an opioid following low-risk surgery.[73] Of the opioids prescribed postoperatively, patients reported 42-71% of tablets went unused due to achieving adequate pain control or the pain stopping altogether before the entire prescription was used.[74] Over prescription is a significant factor to the many instances of abuse and misuse, with more than 90% of the tablets originating from medical providers. Of those who reported misusing opioids, more than half claimed

to have obtained them from a friend or relative,[75] which can be linked to the lack of instructions on how to dispose of unused medication as well as unsecure storage.

Opioids are commonly used due to their potency and effectiveness in analgesia. Unlike non-opioid pain killers, opioid receptors are found on neurons in the peripheral nervous system (PNS)[76] as well as the central nervous system (CNS)[77], allowing them to act in different dispersed physiological manners. However, their versatility also imparts their addictive tendencies and therefore the associated danger. Opioids increase the release of endorphins in the brain by inhibiting the production of γ-aminobutyric acid (GABA), which is responsible for the regulation of endorphins.[78] Endorphins give one the feeling of euphoria and the suppression of pain. Patients can develop a dependence or addiction to this feeling and, when used for a long time, the body can slow it's natural production of endorphins, building a tolerance to the drug. These reasons, as well as other personal reasons unique to the patient, are what makes the current opioid monotherapy methods so risky. Efforts have been made in controlling the delivery of opioids (e.g. sustained delivery in a matrix, transdermal, epidural) to reduce adverse effects that occur from systemic delivery, though the avoidance of using opioids all together is preferred. Still, lack of a plausible alternative has impeded the cessation of prescribing opioids for postoperative pain. Opioids are still maintained in developing technology for postoperative pain management, more of which will be discussed in the following paragraphs.

2.3.1.2. Multimodal Analgesia

The main priority of contemporary postoperative pain management is to limit the use of opioids for this cause. As such, the use of different analgesic compounds, or the

combination of has been sought out by medical professionals. Multimodal analgesia is a technique that aims to optimize pain relief by treating pain through various levels along the pathway of nociception while sparing opioids.[79] These techniques are surgery-specific and population based and afford a more personal regimen for analgesia following any procedure. These routes include the exploitation of non-steroidal anti-inflammation drugs (NSAIDs), paracetamol, local anesthetics (LAs), gabapentinoids, ketamine and glucocorticoids.[80] However, lack of strong evidence promoting the use of multiple analgesics versus a single dose has hindered the extensive use of these techniques in clinic.[81]

2.3.1.3. Controlled Pain Management

Post-operative pharmacotherapy is typically achieved dosage forms that make the entirety immediately bioavailable. This method for achieving analgesia has been associated with fluctuating plasma concentrations, systemic adverse effects and poor patient adherence. On the contrary, controlled drug delivery provides the delivery of doses safely to the specific area of injury. Controlled release (CR) systems include devices that provide extended release (ER), sustained release (SR), delayed release (DR) and targeted release (TR). Controlled delivery systems can be administered in many different ways, each proving their unique individual worth.

2.3.1.3.1. Oral Dosage Models.

The least invasive and perhaps most popular method to date has been oral models. Oral pills/tablets/capsules can be formed with various methods, such as compression

molding, 3-D printing, extrusion, and coating to name a few. In these systems, an active pharmaceutical ingredient (API) is typically homogenously mixed into a matrix of controlled release agent(s) to be released *via* diffusion or degradation of the matrix once introduced to an external environment.

MSContin®, an oral ER dosage form of morphine sulphate, is an example of a controlled release formulation that has already been implicated and shown promising results in comparison to non-controlled methods.[82] In this method, the opioid is blended in both hydrophilic (hydroxypropyl methylcellulose) and hydrophobic polymer (hydroxyl ethyl cellulose) in order to promote both quick and sustained release, respectively. Alike this device, many other commercially available oral dosage forms for the delivery of opioids exist. However, the oral administration route still introduces the potential for adverse effects due to systemic exposure of the opioid (Figure 2.3). By not controlling where the drug takes effect, the bioavailability to the injured area is limited. Moreover, not many drugs are suitable for oral drug delivery due to degradation in the acidic environment of the stomach or intestines, first pass metabolism, or compliance issues with processing. Local delivery of drug directly to the injured site has been introduced to solve many of these issues.

2.3.1.4. Injectable Controlled Release Methods.

One way to achieve more localized drug delivery is intravenous (IV) injection, which has been explored in the form of both gel matrices and nano- or micro-particles.[83,84] IV delivery bypasses some of the issues that arise with oral delivery models such as the

first pass metabolism, degradation, and solubility and bioavailability issues. Most injected systems are able to maintain drug delivery to the affected site of injection.

Injectable doses are a minimally invasive and quick form of controlled delivery. Due to the high surface area of the systems, release is often relatively quick with total delivery usually within a week, though this can be prolonged depending on the fabrication methods. Nevertheless, for post-operative pain management, this time frame is ideal as proper analgesia within the first 3-5 days following the procedure has shown to improve patient healing and recovery.

However, this route does introduce some disadvantages, such as sterility and storage stability, is more invasive that oral or transdermal delivery, and would likely be administered by a physician. Moreover, intravenous controlled release methods have raised concern in regard to the adverse effects in patients due to systemic exposure of the microparticles or injectable components as well as loss of patient compliance due to a fear of needles or other factors.

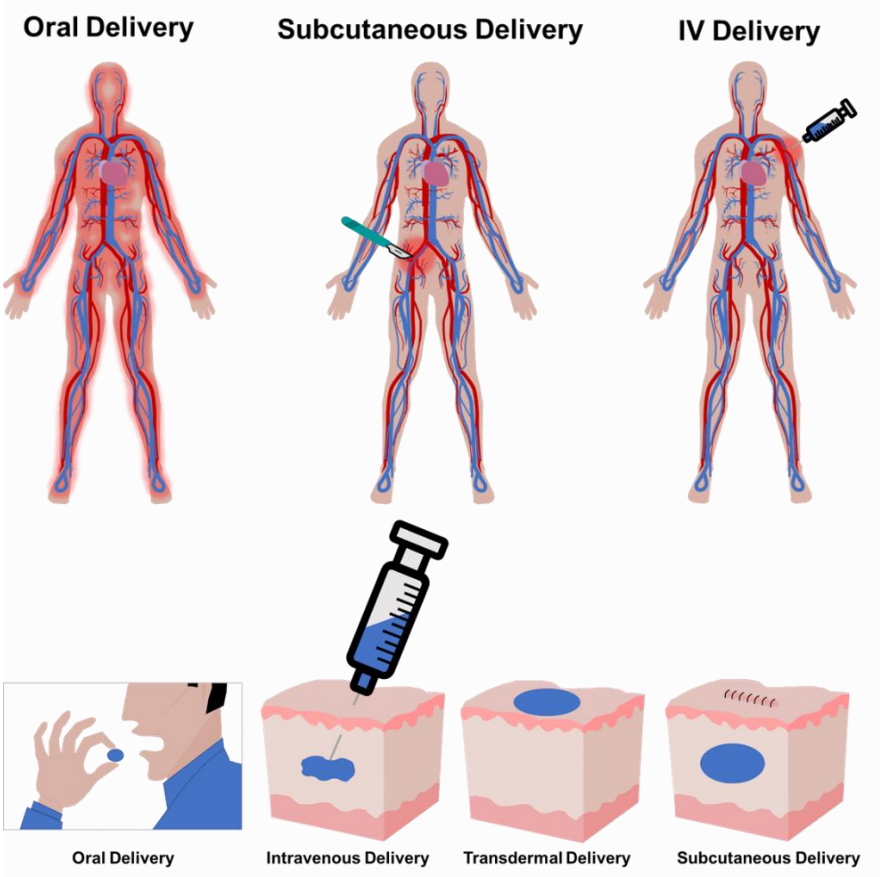

Figure 2.3. Administration methods for common drug delivery techniques. Oral drug delivery induces systemic delivery of drug, exposing the entire bloodstream to the drug. Local drug delivery devices, such as subcutaneous and intravenous (IV) delivery on the other hand, only delivers drug to the infected area.

2.3.1.5. Transdermal Controlled Release Methods.

Transdermal systems on the other hand remove the invasive nature that is imparted by IV injections as well as provides a route in which gastrointestinal drug degradation is not an issue. In an over-the-counter example, transdermal delivery systems have been implemented with lidocaine in the form of pain-alleviating patches. These systems are intended to relieve soreness or pain as a specific area for up to 3 hours. Although effective, this patch, as well as most transdermal methods, run in to the issue of drug solubility and bypassing the skin barrier. Therefore, there are drug requirements

to ensure that the medication gets passed the skin (hydrophilicity, molecular weight, etc.). Additionally, a lag time has been associated with the transdermal mechanisms, which introduces inefficacious delivery of drug to the patient for that time as well as the potential for adverse effects to persist after patch removal.[85] In light of this, more recent work has been examining the effectiveness transdermal delivery systems in which an external stimulus (e.g. iontophoresis) is triggered to release drug[86] or by use of microneedles.[87]

2.3.1.6. Implantable Controlled Release Methods.

The most invasive, yet effective way that has been implemented to achieve controlled drug delivery is the use of implantable devices. Both active and passive implantable drug delivery systems have been explored in the literature, offering various levels of control over drug delivery and also durability of the device.[20] Active systems are energy dependent and require an external trigger to deliver the drug, such as a pump or electric impulse. Passive systems however, delivery drug based on simple drug diffusion and will be the focus herein. These systems maintain the therapeutic at the site of injury and provide relief only to the tissue most local to the implant as the drug is released (Figure 2.3).

In any implant, drug release is dictated by either diffusion from the matrix or degradation of the material.[85,88,89] Depending on the intended length of therapy, biodegradable and non-biodegradable devices have been examined for implantable devices.[20] Non-biodegradable polymers (silicones, polyurethanes, polyacrylates, poly(ethylene vinyl acetate) are often used for contraception and provide longer term release, but require removal at a later time. Alternatively, biodegradable polymers (PCL,

PLA, PLGA) can also be tailored to degrade over a long period of time, offering a lengthened time for therapeutic relief. However, long-term implantation could trigger adverse effects, such as formation of a biofilm and infection, could occur so the safety of the implant over a long period of time must be demonstrated. Specifically, for pain management, the lifetime of the device would need to be short (up to a month), and therefore only biodegradable polymers will be considered.

With the CR mentioned systems, analgesic release occurs at a strictly defined rate, which cannot always match the fluctuating needs of the patients. Controlled pain management should be easily tunable for individuals in terms of how long the drug should act for, how much should be released, and the rate at which this needs to occur to remain efficacious. Some current systems were listed above, but in general, biopolymers, inorganic compounds, and synthetic polymers have been at the forefront of controlled drug delivery.

2.4. Hypothesis and Project Design

The ideal drug delivery device for postoperative pain management would need to combine the beneficial properties listed above. Specifically, the material should be biodegradable, so as not to introduce the need for subsequent removal from the body, contain tunability to achieve personalized dose and duration of analgesia depending on the patient, and possess mechanical properties that align well with the biological site of insertion. Most importantly, the byproducts that will be produced by the polymer degradation must not introduce adverse effects such as inflammation. These ideals can be imagined in various different fabrication methods such as injectable dosages (micro/nano-particles or gels) or implantables (films, meshes, filaments).

Herein, an implantable PEU film will be proposed as an alternative to current post-operative pain management techniques. Given the previous results of PEU films for hernia repairs, these films will not introduce any adverse effects from inflammatory response.[69] As a new concept, a non-opioid analgesic compound will be imbedded in the matrix to be released at a controlled and sustained rate. The release rate can be altered for the intended application (i.e. the severity of pain) by tailoring the fabrication methods accordingly. Factors that are available for analysis include drug-load, polymer composition, and film thickness. Moreover, to show the flexibility of this method, a multi-modal analgesia model will be analyzed.

CHAPTER III

EXPERIMENTAL

3.1. Materials

1,10-decanediol, 1,8-octanediol, 1,6-hexanediol, sodium carbonate, *p*-toluenesulfonic acid monohydrate, and triphosgene were purchased from Sigma Aldrich (Milwaukee, WI). Toluene, chloroform, acetone, and *N*,*N*-dimethylformamide were purchased from Fischer Scientific (Pittsburgh, PA). *L*-valine and *L*-phenylalanine were purchased from Acros (Pittsburgh, PA). Etoricoxib was provided by Merck & Co. Inc. (Rahway, NJ) and Bupivacaine was purchased from Santa Cruz Biotechnology Inc. (Dallas, TX). All solvents were reagent grade and all chemicals were used without further purification unless otherwise stated.

3.2. Characterization

Proton (^{1}H) NMR spectra were obtained using a 300 MHz Varian NMR spectrometer. Chemical shifts are reported in ppm (δ) and referenced to residual solvent resonances (^{1}H NMR DMSO-d_6 2.50 ppm). Multiplicities were explained using the following abbreviations: s = singlet, d = doublet, t = triplet, br = broad singlet, and m = multiplet. Size exclusion chromatography (SEC) was performed using an EcoSEC HLC-8320GPC (Tosoh Bioscience, LLC) equipped with a TSKgel GMHHR-M 7.8mm I.D.×30

cm mixed bed column equipped with a refractive index (RI). The number average molecular mass (M_n), weight average molecular mass (M_w), and molecular mass distribution ($Đ_M$) for each sample was calculated according to a calibration curve of poly(styrene) standards (PStQuick MP-M standards, Tosoh Bioscience LLC) with DMF as the eluent (1.0 mL/min at 50 °C). Differential scanning calorimetry (DSC) was performed using a TA Q200 with heating and cooling cycles (20 °C/min) with temperature sweeps from 0 to 100 °C. The glass transition temperature (T_g) was determined from the midpoint of the second heating cycle curve. Thermogravimetric analysis (TGA) was performed using a TA Q500 with heating ramps of 20 °C/min in the temperature range from 0 to 500 °C/min. The degradation temperature (T_d) was determined from 10% mass loss. Drug-containing solutions were run in an Agilent 1290 Infinity high-pressure liquid chromatograph System (HPLC) and drug concentration was determined using Empower Software (Waters). See Appendices A-C for characterization data.

3.3. Synthesis of Materials

3.3.1. Synthesis of Di-p-toluenesulfonic Acid Salts of Bis(L-valine)-Octane 1,8-Diester Monomer (1-VAL-8).

Synthesis of di-*p*-toluenesulfonic acid salts of bis(*L*-valine)-octane 1,8-diester (1-VAL-8) was carried out according to previously published procedures.[69] Briefly, in a 2 L round bottom flask, 1,8-octanediol (40 g, 0.28 mol, 1 eq.), *L*-valine (74 g, 0.63 mol, 2.25 eq.), *p*-toluenesulfonic acid monohydrate (126 g, 0.65 mol, 2.32 eq.), and toluene (1000 mL) were added and equipped with a stir bar. A Dean-Stark trap attached with a condenser was fastened to the round bottom flask and the reaction was heated to 110 °C and allowed

to reflux for 24 h. The reaction was cooled to room temperature, and the resulting white precipitate was isolated by vacuum filtration using a Buchner funnel. The product was dissolved in boiling water (2 L), hot vacuum filtered, and cooled to room temperature to purify the white solid precipitate. The precipitate was collected via filtration and the recrystallization process was performed three times for purity. ^{1}H NMR (300 MHz, 303 K, DMSO-d_6): δ = 0.91-0.97 (m, 12H), 1.28 (s, 8H), 1.59 (m, 4H), 2.10-2.21 (m, 2H), 2.27 (s, 6H), 2.50 (m, DMSO), 3.83-3.84 (d, $^{3}J_{H\text{-}H}$ = 4.4 Hz, 2H), 4.05-4.15 (m, 4H), 7.07-7.09 (d, $^{3}J_{H\text{-}H}$ = 7.9 Hz, 4H, aromatic H), 7.43-7.46 (d, $^{3}J_{H\text{-}H}$ = 9.9 Hz, 4H, aromatic H), 8.27 (br, 6H) ppm.

3.3.1.1. Synthesis of Di-p-toluenesulfonic Acid Salts of Bis(L-Valine)-Decane 1,10-Diester Monomer. (1-VAL-10).

Synthesis of the di-p-toluene sulfonic acid of bis(*L*-valine)-decane 1,10-diester (1-VAL-10) was carried out using the method described above. ^{1}H NMR (300 MHz, 303 K, DMSO-d_6): δ = 0.93-0.99 (m, 12H), 1.26 (s, 8H), 1.58-1.62 (m, 4H), 2.09-2.17 (m, 2H), 2.29 (s, 6H), 2.50 (m, DMSO), 3.17-3.36 (s, H_2O), 3.91-3.93 (d, $^{3}J_{H\text{-}H}$ = 4.5 Hz, 2H), 4.08-4.24 (m, 4H), 7.11-7.13 (d, $^{3}J_{H\text{-}H}$ = 7.9 Hz 4H, aromatic H), 7.44-7.47 (d, $^{3}J_{H\text{-}H}$ = 7.6 Hz4H, aromatic H), 8.29 (br, 6H) ppm.

3.3.1.2. Synthesis of Di-p-toluenesulfonic Acid Salts of Bis(L-phenylalanine)-Hexane 1,6-Diester Monomer. (1-PHE-6).

Synthesis of di-*p*-toluene sulfonic acid of bis(*L*-phenylalanine)-hexane 1,6-diester (1-PHE-6) was carried out using the method described above. ^{1}H NMR (300 MHz, 303 K,

DMSO-d_6): δ =1.05 (s, 4H), 1.38 (m, 4H), 2.29 (s, 6H), 2.50 (m, DMSO), 2.97−3.20 (m, 4H), 3.36 (s, H_2O), 3.99-4.03 (t, $^3J_{H\text{-}H}$ = 6.4 Hz, 4H), 4.27-4.31 (m, 2H), 7.11−7.14 (d, $^3J_{H\text{-}H}$ = 7.9 Hz, 4 H), 7.21−7.35 (m, 10H), 7.48−7.51 (d, $^3J_{H\text{-}H}$ = 7.9 Hz, 4H), 8.44 (s, 6H) ppm.

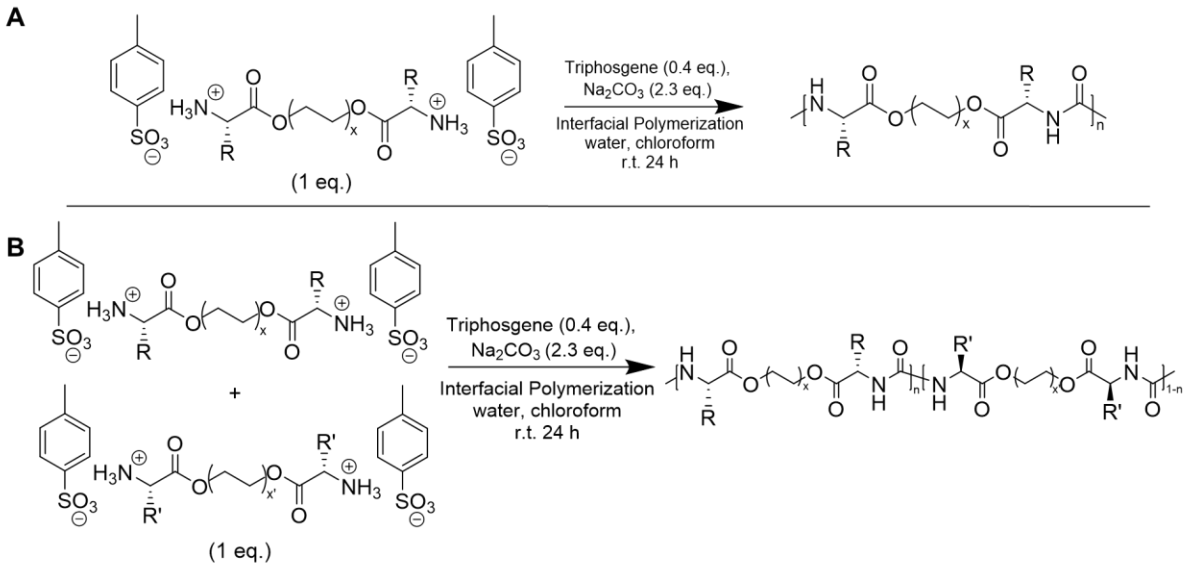

Scheme 3.1. Synthetic route for the formation of poly(ester urea)s *via* interfacial polymerization. Homopolymer was synthesized with one composition of monomer salt (1 eq.) dissolved in water followed by the addition of triphosgene (0.4 eq) in chloroform (A). Sodium carbonate (2.3 eq.) is added to deprotonate the amine salts, in turn readily forming the urea moiety. PEU copolymers are synthesized in a similar fashion, but with the addition of two compositions of monomer salts (B).

3.3.2. Synthesis of Poly(ester urea) Homopolymers and Copolymers.

The synthesis of all polymers was adapted according to previous literature.[90] Briefly, an interfacial polymerization of *p*-toluenesulfonic acid monomer salts was performed by dissolving the monomers with desired molar equivalents (1 eq. total) with sodium carbonate (3.1 eq.) in distilled water (0.25 M Na_2CO_3, 35 °C) in a 5 L 3-neck round-bottom flask. The solution was equipped with an overhead mechanical stir rod and

allowed to stir until clear. The reaction was then placed in an ice bath and cooled to 0°C. In a 500 mL round bottom flask, triphosgene (0.40 eq.) was dissolved in chloroform (0.20-0.21 M, r.t.) and subsequently poured to the reaction vessel slowly. The solution turned white upon addition of the chloroform mixture and was stirred for 24 hours. The product was then transferred to a separatory funnel. The reaction mixture was precipitated into boiling water to remove chloroform and starting material impurities. The polymer was collected, frozen in liquid nitrogen, and then dried under reduced pressure to remove residual water.

3.3.2.1. *Poly[(1-VAL-10)]* (V10) ^{1}H NMR (300 MHz, 303 K, DMSO-d_6): δ = 0.81-0.87 (m, 12H, -CH(C**H**$_3$)$_2$), 1.95-2.01 (m, 2H, -NHCH(C**H**(CH$_3$)$_2$)C(O)O-), 6.37-6.40 (d, $J_{H\text{-}H}$ = 8.8 Hz, 2H, -N**H**CH(CH(CH$_3$)$_2$)C(O)O-), 1.24, 1.53, 4.01-4.14 (all remaining diol protons). (M_w = 217 kDa, M_n = 143 kDa, $Đ_m$ = 1.5, T_g = 42 °C, T_d = 275 °C) (50-58% yield).

3.3.2.2. *Poly[(1-VAL-8)$_{0.70}$-co-(1-PHE-6)$_{0.30}$]*. (30P6V8). ^{1}H NMR (300 MHz, 303 K, DMSO-d_6): δ = 0.81-0.87 (m, 12H, -CH(C**H**$_3$)$_2$), 1.93-1.99 (m, 2H, -NHCH(C**H**(CH$_3$)$_2$)C(O)O-), 2.90-2.92 (m, 4H, -NHCH(C**H**$_2$Ph**)**C(O)O-), 4.35-4.40 (m, 2H, -NHC**H**(CH$_2$Ph**)** C(O)O-), 6.36-6.39 (d, $J_{H\text{-}H}$ = 9.2 Hz, 2H, -N**H**CH(CH(CH$_3$)$_2$)C(O)O-), 6.49-6.52 (d, $^{3}J_{H\text{-}H}$ = 8.9 Hz, 2H, -C(O)N**H**C(CH$_2$Ph**)**HC(O)-), 7.16-7.25 (m, 10H, -C$_6$**H**$_5$**)**, 1.18-1.25, 1.45-1.53, 3.97-4.03 (all remaining diol protons) ppm. (M_w = 104 kDa, M_n = 52 kDa, $Đ_M$ = 2.0, T_g = 45 °C, T_d = 263 °C) (81-90% yield).

3.3.2.3. *Poly[(1-VAL-8)$_{80}$-co-(1-PHE-6)$_{20}$]*. (20P6V8). ^{1}H NMR (300 MHz, 303 K, DMSO-d_6): δ = 0.82-0.85 (m, 12H, -CH(C**H**$_3$)$_2$), 1.95-2.02 (m, 2H, -NHCH(C**H**(CH$_3$)$_2$)C(O)O-), 2.89 – 2.97 (m, 4H, -NHCH(C**H**$_2$Ph**)**C(O)O-), 4.35-4.42 (m, 2H, -NHC**H**(CH$_2$Ph**)** C(O)O-), 6.37-6.40 (d, J_{H-H} = 9.2 Hz, 2H, -N**H**CH(CH(CH$_3$)$_2$)C(O)O-), 6.50-6.53 (d, $^3J_{H-H}$ = 9.0 Hz, 2H, -C(O)N**H**C(CH$_2$Ph**)**HC(O)-), 7.15-7.30 (m, 10H, -C$_6$**H**$_5$), 1.19-1.26, 1.46-1.54, 3.97-4.06 (all remaining diol protons) ppm. (M_w = 88 kDa, M_n = 56 kDa, $Đ_M$ = 1.6, T_g = 57 °C, T_d = 278 °C) (73-81% yield).

3.3.2.4. *Poly[(1-VAL-8)$_{90}$-co-(1-PHE-6)$_{10}$]*. (10P6V8). ^{1}H NMR (300 MHz, 303 K, DMSO-d_6): δ = 0.82-0.87 (m, 12H, -CH(C**H**$_3$)$_2$), 1.97-2.00 (m, 2H, -NHCH(C**H**(CH$_3$)$_2$)C(O)O-), 2.89-2.97 (m, 4H, -NHCH(C**H**$_2$Ph**)**C(O)O-), 4.33-4.39 (m, 2H, -NHC**H**(CH$_2$Ph**)** C(O)O-), 6.37-6.40 (d, J_{H-H} = 8.9 Hz, 2H, -N**H**CH(CH(CH$_3$)$_2$)C(O)O-), 6.50-6.53 (d, $^3J_{H-H}$ = 9.3 Hz, 2H, -C(O)N**H**C(CH$_2$Ph**)**HC(O)-), 7.15-7.29 (m, 10H, -C$_6$**H**$_5$), 1.18-1.26, 1.45-1.54, 3.96-4.03 (all remaining diol protons) ppm. (M_w = 107 kDa, M_n = 68 kDa, $Đ_M$ = 1.6, T_g = 44 °C, T_d = 245°C) (68-73% yield).

3.3.3. *Blade Coating PEU Films*.

Polymer solutions of V10, 10P6V8, 20P6V8, and 30P6V8 were prepared by dissolving 25-45% of polymer in acetone (w/w) to obtain variety in final film thickness. Drug loadings were 20 or 40% etoricoxib by weight (drug/polymer) and 10% bupivacaine and etoricoxib each for combination films. The solution was left for 24 hours in an incubator (37°C, 80 rpm) to afford the homogenous mixture. Once thoroughly mixed, solutions were fed into a well where a polyethylene terephthalate (PET) substrate and a Doctor blade (gap height of

0.5-1 mm) were stationed (Scheme 3.2A). Using an EC-100 Fixed Speed Drawdown Coater, the doctor blade was pushed, drawing the solution cast film out onto the substrate as shown from the front (Scheme 3.2B) and from the side (Scheme 3.2C). Films were dried for a minimum of 24 hours under ambient conditions to allow for the film to set with minimal defects and dried further by freeze-drying and lyophilization to ensure that residual solvent had been removed prior to additional testing. Film thickness was measured using calipers at various locations across the film to ensure a uniform thickness and to obtain an average (n = 4).

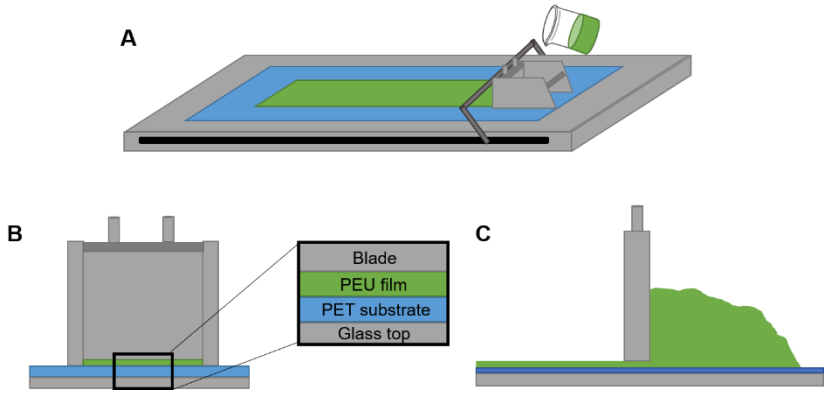

Scheme 3.2. Film fabrication through blade-coating where (A) polymer solutions are poured into the well of a doctor blade that is then pulled by a drop down lever, leaving behind a film of the polymer solution (green) on top of a PET substrate (blue). The height of the doctor blade can be changed to give different film thickness by adjusting the screws on the top (B). A side view of this process and the polymer solution in the doctor blade well is shown in (C).

3.3.4. *Drug Content Uniformity*.

Samples were taken from different sections of the solution cast films. The films were placed in a 50:50 mixture of ethanol/THF and sonicated in a water bath (45 °C). Samples were diluted with equal amounts of phosphate buffer to the organic mixture and etoricoxib content was quantified using an Agilent 1290 Infinity high-pressure liquid chromatograph system equipped with a UV-Vis detector (HPLC). Drug content from each

sample was then taken and averaged to give the amount of etoricoxib in each film. This value was then compared to a theoretical value (calculated by the weight of the film multiplied by the drug loading) and the accuracy of the theoretical method was considered. Theoretical accuracy was determined by:

$$Theoretical\ Accuracy\ (\%) = \frac{Theoretical\ amount\ of\ etoricoxib\ (mg)}{Actual\ amount\ of\ etoricoxib\ (mg)}\ x\ 100$$

This process was also carried out for the films used for release after they were retired from the study (n = 3) to get an accurate measure of the cumulative drug release (%).

3.3.5. *In Vitro Drug Release*.

Films were blade coated as described above and samples were cut out using a razor blade. The exact mass and thickness of each sample was measured using a laboratory balance and calipers respectively. Drug release experiments were conducted on 2 cm square sections of the polymer films in two different ways. The combination films of etoricoxib and bupivacaine were weighed down the placed in phosphate buffer solution (1 x PBS) to prevent the films from floating. The vials were then placed in an incubator (37 °C) and shaken at 100 rpm. Alternatively, the etoricoxib films were placed into magnetic baskets that were then placed into the vessels of an Agilent USP Apparatus 7 equipped with an auto-sampler (Merck & Co., Inc.). The vessels were filled with 10 mL of Dulbecco's phosphate-buffered saline (dPBS) and samples were taken at programmed time points; etoricoxib release was monitored over 7-14 days. The agitation rate of the vessels was 40 dips per minute (DPM) and the baths were kept at 37 °C. The entire media volume

was replaced after each sample collection for both methods. Once collection was finished, the samples were analyzed using HPLC analysis. Once retired from the study, the remaining etoricoxib in the film was determined by the methods described above.

3.3.6. *In Vivo Release Model of Etoricoxib from PEU Films.*

All animal studies were performed in house at Merck & Co. Inc. (Rahway, NJ) upon approval. Films of 10P6V8 and 30P6V8 were prepared by measuring out a film that contains approximately 9 mg of etoricoxib based on the theoretical prediction method (150-250 mm). Samples were then gamma irradiated to ensure proper sterilization for implantation. Once ready, 12 rats were prepared by shaving the site scapular region where the incision was made (n = 6 per sample set). To create a pocket for the film, a hemostat was placed and opened, leaving a spot for the film to be inserted. The surgical site was then sutured and drug release was monitored at specific time points through the tail vein through 11 days. At the completion of the study, the rats were sacrificed and the surrounding tissue was collected along with the film to test for etoricoxib content that stayed local to the implant. This value was then compared to how much etoricoxib was delivered systemically (to the blood stream) to determine the extent of local drug delivery).

3.3.7. *Statistical Analysis.*

Statistical analysis between sample sets were done using Tukey one-way ANOVA to analyze differences between multiple sets with respect to drug-load, polymer composition, or film thickness on drug release at day 7. Data is reported as means ± standard error. A $p<0.05$ was considered statistically significant.

3.3.8. *Release Kinetics.*

To more accurately understand the underlying mechanism of etoricoxib release from the films, the data was fit to the Higuchi model.[91] This model allows for an approximate determination of diffusivity constant as well as a prediction for total release, which allows for a quantitative comparison between films.

CHAPTER IV

RESULTS & DISCUSSION

Thus far, an economical and efficient blade-coating technique has been utilized that affords control over the film dimensions (e.g. thickness, shape, and size) to attain drug-loaded poly(ester urea) (PEU) matrices with various drug-loads and polymer compositions. Considering all these variables, patient or property specific films are possible. The application of this research could be advantageous in considering these films as post-operative implants for direct analgesia at the surgical site to limit the need for oral prescriptions. The polymers used were selected for their previous indications as a material that did not produce notable inflammation *in vivo* as well as for their mechanical and physical properties. [90,92] In this study, little to no inflammation of the implantation site was noted. Furthermore, the release of drug followed a continuous curve, indicating that no acidic environment was created in the soft tissue, triggering degradation to hasten the drug release and cause erratic patterns.

4.1 Content Determination of Etoricoxib Films.

Punches from each blade-coated film were measured and dissolved as described in the methods above to test for the remaining etoricoxib content via HPLC. The amount obtained from this process was assumed to be the actual etoricoxib amount. Theoretical values for etoricoxib content was calculated according to the weight of the film and the

intended drug-load (weight of drug/weight of polymer); this calculation assumes a homogeneous distribution of drug in the film. The predicted value was then compared to the actual etoricoxib amount calculated to quantify the accuracy of the theoretical method (Table 4.1). As can be noted, the estimation of etoricoxib content in the film deviates from the actual value. This was attributed to minimal drug aggregation in areas of the film that were cut out for testing. Drug aggregation is likely due to differences in chain stacking and, accordingly, drug interactions with the chain. A possible solution to this employs better mixing of the viscous drug/polymer solution prior to blade-coating to ensure an even distribution of etoricoxib. Considering this hurdle, all films that were run for drug release were also dissolved once the dissolution was completed to get accurate cumulative label claim for the duration of the release.

Table 4.1. Content of etoricoxib in each set of films. Theoretical (predicted based on the weight of the film and the drug loading) values were compared to the actual amount of etoricoxib calculated according to HPLC analysis. The accuracy of the theoretical predicted value was determined by obtaining a percentage of the theoretical drug load versus the actual drug load. Variations were attributed to aggregation of drug in the specific area that was sectioned from the film. * indicates samples sets only containing n=2, all other sets were n=3.

Polymer	Drug Load (%)	Theoretical Amount (mg)	Actual Amount (mg)	Theoretical Accuracy (%)
P(1-VAL-10)*	20	5.1 ± 1.5	4.7 ± 1.8	109.9 ± 9.3
P(1-VAL-10)*	40	11.3 ± 2.7	10.6 ±2.2	106.8 ± 3.1
30% 1-PHE-6 P(1-VAL-8)*	20	4.5 ± 0.4	3.9 ± 0.2	110.7 ± 19.6
30% 1-PHE-6 P(1-VAL-8)*	40	7.6 ± 0.7	5.8 ± 0.6	131.5 ± 1.9
10% 1-PHE-6 P(1-VAL-8)	20	7.6 ± 1.5	7.6 ± 1.9	100.5 ± 9.5
20% 1-PHE-6 P(1-VAL-8)*	20	5.4 ± 0.3	7.5 ± 2.1	77.0 ± 20.2
30% 1-PHE-6 P(1-VAL-8)	20	4.8 ± 1.1	4.0 ± 1.0	120.8 ± 10.1
P(1-VAL-10)	20	3.8 ± 1.4	3.0 ± 0.6	122.0 ± 19.0

*indicates n = 2

4.2. In Vitro Etoricoxib Release from Poly(ester urea) Films.

To gain insight on the release behavior of etoricoxib from PEU films, a diffusion test was carried out in Dulbecco's phosphate-buffered saline (dPBS). Overall, the release curves of each polymer and drug loading reveal a sustained release of etoricoxib. Although none of the films reach full drug release over the period analyzed, they would be expected to go to completion if left for a longer study. Furthermore, the release profile maintains continuity over time, suggesting it is dictated by one, primary event (e.g. diffusion). In contrast, previous literature of poly(lactide-co-glycolide) (PLGA) films has reported curves with multimodal release likely attributed to the bulk degradation of PLGA and therefore, a nonlinear increase in drug release from the polymer matrix.[93,94] These results indicate that PEUs could offer a more predictable and controllable release of drug *in vitro.* Moreover, full release of drug from each film was estimated by fitting the release data to the Higuchi model,[91,95] the discussion of which will follow. Overall, differences in etoricoxib release varied with drug loading, film polymer composition, and thickness.

Table 4.2. Characterization of blade-coated 30% 1-PHE-6 P(1-VAL-8) (30P6V8) and P(1-VAL-10) (V10) blade-coated films for release studies. Both polymers were prepared with different drug loadings (20% and 40% (w/w) etoricoxib) and etoricoxib content was calculated based on the intended drug-load and the initial weight of the film (theoretical value). Measured were taken and averaged (n = 3).

Polymer	Drug-load (%)	Thickness (μm)	Weight of film (mg)	Etoricoxib content (mg)
30% 1-PHE-6 P(1-VAL-8)	20	84	21.1 ± 0.6	4.2 ± 0.1
30% 1-PHE-6 P(1-VAL-8)	40	84	21.7 ± 2.7	8.7 ± 1.1
P(1-VAL-10)	20	85	18.2 ± 1.0	3.6 ± 0.2
P(1-VAL-10)	40	100	25.0 ± 2.9	10.0 ± 1.1

4.2.1. *Effect of Drug-load on Drug Release.*

Two different drug-loads (20% and 40% (w/w) etoricoxib) were used with 30% 1-PHE-6 P(1-VAL-8) (30P6V8) and P(1-VAL-10) (V10) films to observe differences in diffusion of drug from the polymer matrix. Films were coated at the same speed and gap height in the doctor blade to maintain a consistent thickness (Table 4.2) and film sections were cut into 2 cm squares.

Drug release profiles indicate that there are differences when drug-load is varied (Figure 4.1). Specifically, when percent label claim was considered, higher drug-loaded films (40% etoricoxib) were released slower through day 7 in comparison to the 20% drug-load (Table 4.3). This result correlates well as changes in drug distribution throughout the film as the amount of drug is increased could be expected. In the higher drug loaded films, more etoricoxib must be packed into the same area, causing an inhomogeneity of drug at the surface to drug in the bulk in comparison to lower drug loaded films. This difference in distribution proves fruitful for pain management applications as more homogeneous drug loads will produce a prolonged anesthetic effect by releasing drug for a longer time (i.e. drug in the bulk of the film will take longer to diffuse out). Slower release models could be of great use for pain that is more chronic and persistent.

4.2.2. *Effect of Polymer Composition on Drug Release.*

10% 1-PHE-6 P(1-VAL-8) (10P6V8), 20% 1-PHE-6 P(1-VAL-8) (20P6V8), 30% 1-PHE-6 P(1-VAL-8) (30P6V8), and P(1-VAL-10) (V10) films were prepared at 20% etoricoxib (w/w) and analyzed for the effect of polymer composition on drug release. Films were coated at the same speed and gap height in the doctor blade (Table 4.4) and sections

were cut in 2 cm squares. Slight variation was shown between films and average thickness. To account for this, the effect of thickness on drug release was also studied, the results of which will follow.

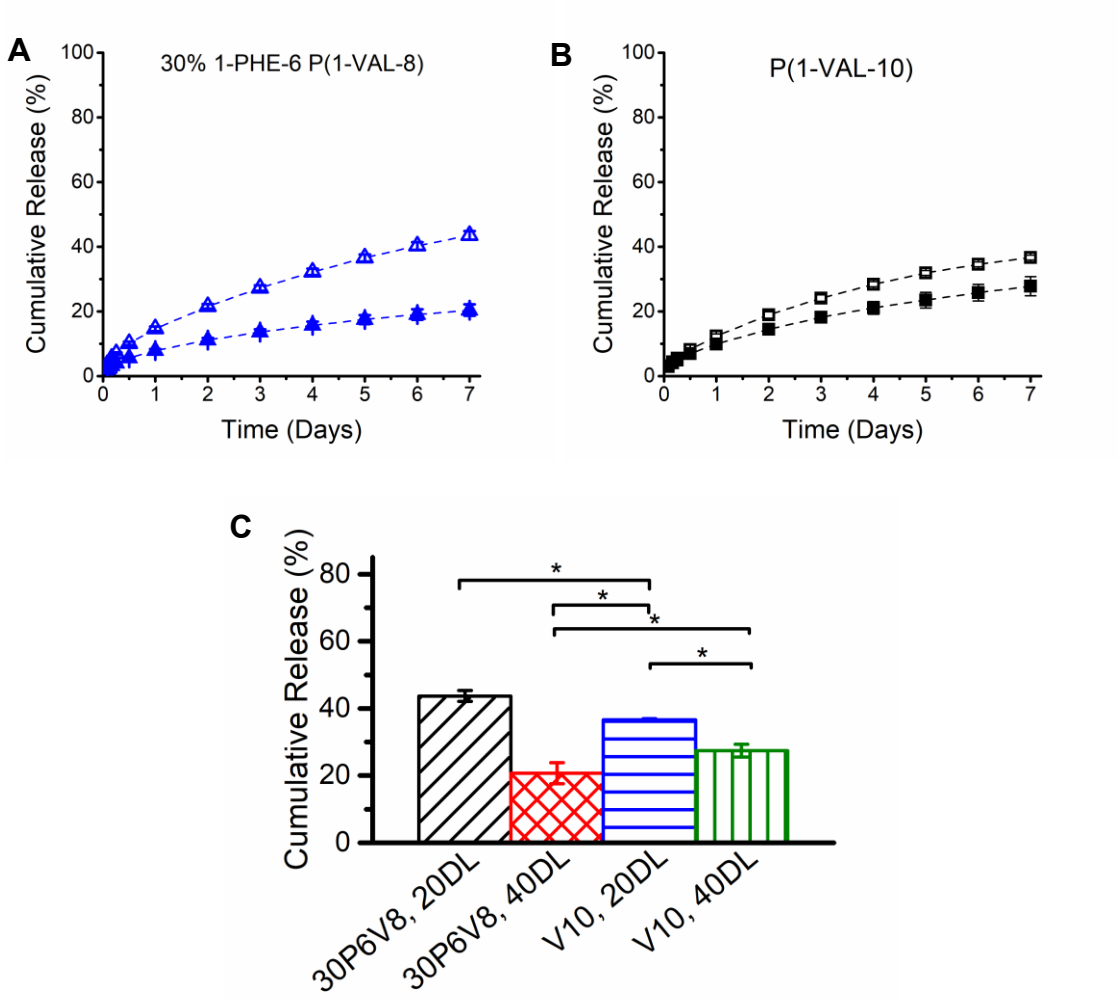

Figure 4.1. Release curves of etoricoxib-loaded PEU films. (A) 30% 1-PHE-6 P(1-VAL-8) and (B) P(1-VAL-10) were tested at 20% (empty shapes) and 40% (filled shapes) drug-loading. All films were tested in an Agilent 400-DS Dissolution Apparatus 7 at 37 °C with 40 DPM. Cumulative release (%) was calculated according to the remaining amount of etoricoxib in the film after it was retired from the study. Values for total release on day 7 were compared between samples by a Tukey one-way ANOVA, where $p<0.05$ was considered significant and is indicated by a * (C).

Table 4.3. Release results of various drug-loading films at day 7. Values were taken and averaged (n = 3).

Polymer	Drug-load (%) (w/w)	Release at day 7 (mg)	Release at day 7 (%)
30% 1-PHE-6 P(1-VAL-8)	20	1.48 ± 0.09	43.7 ± 1.2
30% 1-PHE-6 P(1-VAL-8)	40	1.05 ± 0.27	20.7 ± 1.3
P(1-VAL-10)	20	2.80 ± 0.11	36.6 ± 0.7
P(1-VAL-10)	40	1.68 ± 0.45	27.5 ± 2.9

Table 4.4. Characterization of blade-coated 10% 1-PHE-6 P(1-VAL-8) (10P6V8), 20% 1-PHE-6 P(1-VAL-8) (20P6V8), 30% 1-PHE-6 P(1-VAL-8) (30P6V8), and P(1-VAL-10) (V10) films for release studies with 20% (w/w) etoricoxib. Etoricoxib content was calculated based on post-dissolution analysis of the film using total content analysis methods and thicknesses were averaged using calipers. All films were coated at the same gap height on the doctor blade. Values were measured and averaged (n = 3).

Polymer	Drug-load (%)	Thickness (μm)	Weight of film (mg)	Etoricoxib content (mg)
10% 1-PHE-6 P(1-VAL-8)	20	87	40.30 ± 8.72	7.20 ± 1.48
20% 1-PHE-6 P(1-VAL-8)	20	51	26.60 ± 3.80	6.23 ± 0.57
30% 1-PHE-6 P(1-VAL-8)	20	44	27.83 ± 2.46	4.97 ± 0.90
P(1-VAL-10)	20	38	21.23 ± 5.85	4.10 ± 1.35

Overall, release of etoricoxib through 7 days was shown to vary with polymer composition as shown by the comparison of the different phenylalanine-valine copolymers (10P6V8, 20P6V8, and 30P6V8) and V10. All films maintained a continuous release profile (Figure 4.2). At day 7 of release, the label claim released ranged from 33% to 66% depending on the PEU composition and release rates vary accordingly (Table 4.5). The differences observed with polymer composition could be attributed to drug interactions with the polymer chain. Specifically, depending on the two types of amino acids groups analyzed, different intermolecular forces were suggested to be impacting the diffusion of

etoricoxib from the polymer matrix. With the phenylalanine-based copolymers, the presence of an aromatic group could allow for pi-interactions to occur between the etoricoxib and polymer. These interactions are likely why slower release profiles are observed for the phenylalanine analogues when compared to the V10 homopolymer which lacks the aromatic side chain. Additionally, PEUs have been shown previously to display an elaborate hydrogen bonding network through the urea and carbonyl moieties in the backbone.[92,96] Although etoricoxib does not have bountiful hydrogen bond donor groups (i.e. an alcohol or amine) compared to other anesthetics, such as lidocaine and bupivacaine, this interaction could help indicate the sustained release profiles for all PEU materials. Having multiple ways to tune drug release based on drug interactions through chemical composition of the polymer is ideal as it opens the door for other drug release applications and will be analyzed further in future work.

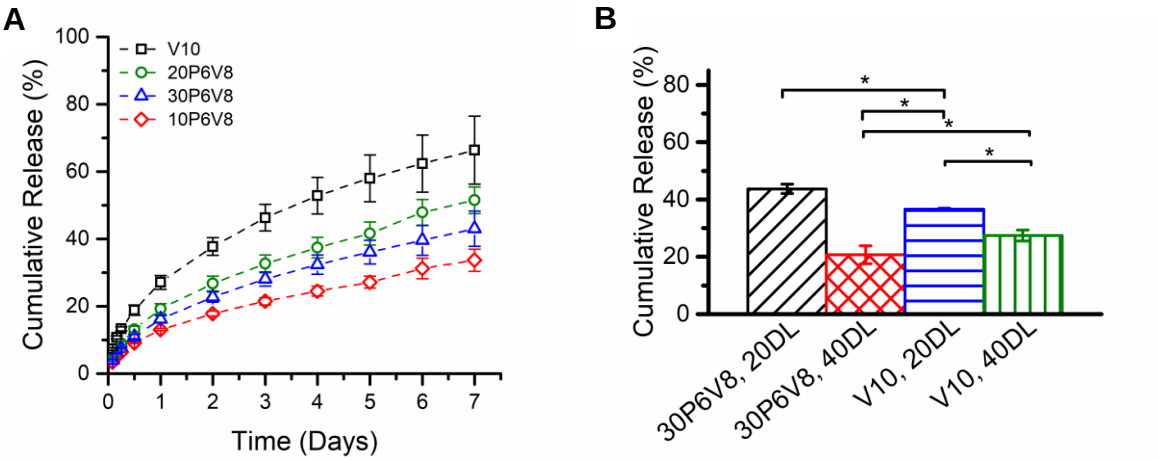

Figure 4.2. Release curves of etoricoxib-loaded PEU blade coated films. 10% 1-PHE-6 P(1-VAL-8) (10P6V8), 20% 1-PHE-6 P(1-VAL-8) (20P6V8), 30% 1-PHE-6 P(1-VAL-8) (30P6V8), and P(1-VAL-10) (V10) were all tested at 20% drug-load. All films were tested in an Agilent 400-DS Dissolution Apparatus 7 at 37°C with 40 DPM. Cumulative release (%) was calculated according to the remaining amount of etoricoxib in the film after it was retired from the study. Values for total release on day 7 were compared between samples by a Tukey one-way ANOVA, where $p<0.05$ was considered significant and is indicated by a * (B).

Table 4.5. Total release data of 10P6V8, 20P6V8, 30P6V8, and V10 films with 20% (w/w) etoricoxib loading at day 7. Values were taken from the time point and averaged (n = 3).

Polymer	Drug-load (%)	Release at day 7	Release at day 7
10% 1-PHE-6 P(1-VAL-	20	2.35 ± 0.24	33.2 ± 3.8
20% 1-PHE-6 P(1-VAL-	20	3.09 ± 0.24	49.8 ± 1.6
30% 1-PHE-6 P(1-VAL-	20	2.05 ± 0.27	41.9 ± 5.4
P(1-VAL-10)	20	2.59 ± 0.40	66.0 ±13.9

4.2.3. *Effect of Film Thickness on Drug Release.*

By varying the concentration of the drug-loaded solution and the gap height of the doctor blade, different film thicknesses were obtained. Altering the thickness of the film changes the distribution of drug within the matrix and, therefore, the ability of the drug to diffuse out of the film. The polymer used for this study was the 30P6V8 copolymer and the etoricoxib load was kept constant at 20%. Thicknesses obtained were 77, 200, and 430 µm. 8 mm circular punches were cut out of the large strip and films were placed in phosphate buffer (37 °C, agitating at 80 rpm) solution to test for release. The full dimensions of these films can be found in Table 4.6.

Table 4.6. Characterization of blade-coated 30% 1-PHE-6 P(1-VAL-8) (30P6V8) films for release studies with 20% (w/w) etoricoxib at various thicknesses. Etoricoxib content was calculated based on post-dissolution analysis of the film using total content analysis methods and thicknesses were averaged using calipers. Solution concentration and gap height of the doctor blade was varied to produce a difference in film thickness (n = 3).

Polymer	Drug-load (%)	Thickness (µm)	Weight of film (mg)	Etoricoxib content (mg)
30% 1-PHE-6 P(1-VAL-8)	20	78	2.07 ± 0.50	0.41 ± 0.10
30% 1-PHE-6 P(1-VAL-8)	20	200	11.37 ± 0.32	2.27 ± 0.06
30% 1-PHE-6 P(1-VAL-8)	20	430	25.70 ± 1.40	5.14 ± 0.28

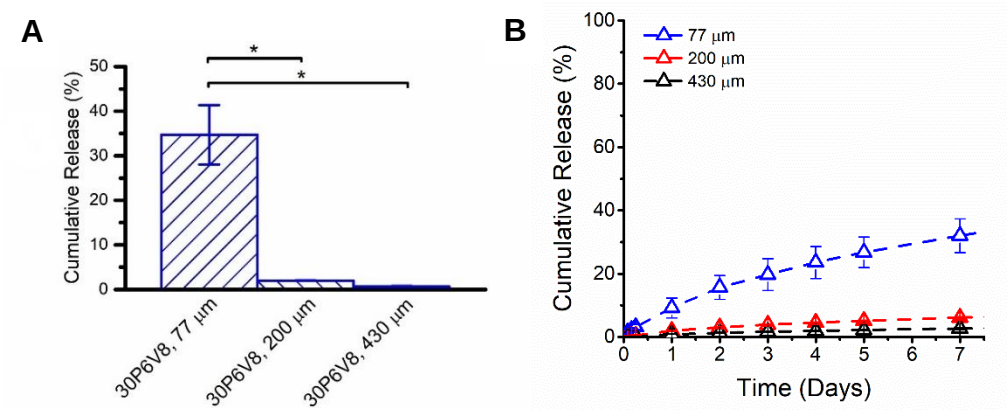

Figure 4.3. Cumulative release curves of 30% 1-PHE-6 P(1-VAL-8) (30P6V8) films with 20% etoricoxib loading at various thicknesses (77, 200, and 430 µm) (A). Films were placed in phosphate buffer solution and kept at 37 °C agitating at 80 rpm. Cumulative release (%) was calculated according to the remaining amount of etoricoxib in the film after it was retired from the study. Values for total release on day 7 were compared between samples by a Tukey one-way ANOVA, where $p<0.05$ was considered significant and is indicated by a * (B).

The release curves indicate that the thicker the film, the longer the duration of anesthesia, or the longer the time for total drug release. Explicitly, these results show that thicker films are able to pack more drug in the shape of the film homogeneously, therefore giving rise to a film that will release etoricoxib at the same rate, but for a longer duration. Moreover, as all of these films release the same amount of drug (Table 4.7), it is fair to say that these films are releasing drug at the same rate (etoricoxib is diffusing out of the film at the same rate) and that etoricoxib is homogeneously distributed at the surface.

Table 4.7. Total release data of 30% 1-PHE-6 P(1-VAL-8) (30P6V8) 20% etoricoxib (w/w) films with different thicknesses. Data is taken from the day 7 time point and all values are triplicate averages.

Thickness (µm)	Drug-load (%) (w/w)	Release at day 7 (mg)	Release at day 7 (%)	Total drug-load (mg)
77	20	0.14 ± 0.01	34.7 ± 6.7	0.41 ± 0.10
200	20	0.13 ± 0.00	2.0 ± 0.4	2.27 ± 0.06
430	20	0.13 ± 0.00	0.7 ± 0.1	5.14 ± 0.28

4.2.4. Release from Bupivacaine and Etoricoxib Loaded Films.

To show that multi-modal analgesia is possible with these films bupivacaine (a local anesthetic) and etoricoxib (an NSAID) were both loaded into PEU films. Bupivacaine works through the sodium channels on the primary afferent neuron and etoricoxib is a selective COX-2 inhibitor, inhibiting the production of the inflammatory mediators, prostaglandin, therefore both these drugs should work in tandem to produce an additive analgesic effect rather than a competitive one. Films were loaded with 10% of each drug (w/w) for a total drug load of 20%. A series of valine-based polymers with various diol chain lengths were used given the rate of etoricoxib release in previous studies (Table 4.8).

Table 4.8. Dimensions of valine-based PEU films loaded with etoricoxib and bupivacaine at 10% (w/w) drug-load each.

Polymer	Drug-load, each (w/w, %)	Thickness (μm)	Weight of film (mg)	Etoricoxib content (mg)	Bupivacaine content (mg)
P(1-VAL-8)	10	177	8.70 ± 1.74	0.87 ± 0.17	0.87 ± 0.17
P(1-VAL-10)	10	110	4.53 ± 0.87	0.45 ± 0.09	0.45 ± 0.09
P(1-VAL-12)	10	160	7.93 ± 0.49	0.79 ± 0.05	0.79 ± 0.05

Etoricoxib and bupivacaine released at about the same rate throughout the study and regardless of polymer composition (Figure 4.4). However, it was evident that the longer the diol chain length, or the more hydrophobic the polymer, the quicker the release of drug from the film to a certain extent. This observation is more apparent between the P(1-VAL-8) and the longer chains, but not as evident when comparing the P(1-VAL-10) to the P(1-VAL-12). Regardless, *in vitro* assessment of multi-modal analgesia models of PEU films were deemed plausible with a consistent rate of release of both etoricoxib and bupivacaine through the polymer hydrophobicity variations.

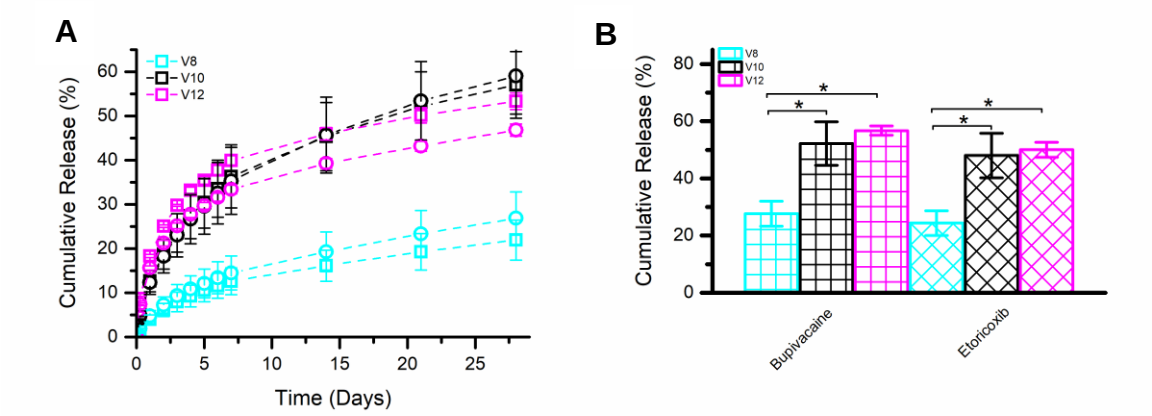

Figure 4.4. Release of etoricoxib (circles) and bupivacaine (squares) from valine-based PEU films. Release was monitored through 7 days (A). Films were placed in phosphate buffer solution and kept at 37 °C agitating at 80 rpm. Cumulative release (%) was calculated according to the remaining amount of etoricoxib in the film after it was retired from the study. Values for total release on day 7 were compared between samples by a Tukey one-way ANOVA, where $p<0.05$ was considered significant and is indicated by a * (B).

Table 4.9. Total release data of valine-based PEU combination films with etoricoxib and bupivacaine at 10% (w/w) drug-load each. Data was taken from the day 7 timepoints and averaged (n = 3).

Polymer	Drug	Release at day 7 (mg)	Release at day 7 (%)
P(1-VAL-8)	Bupivacaine	0.11 ± 0.01	27.7 ± 4.3
P(1-VAL-10)		0.16 ± 0.00	52.2 ± 7.6
P(1-VAL-12)		0.32 ± 0.1	56.7 ± 1.6
P(1-VAL-8)	Etoricoxib	0.12 ± 0.01	24.4 ± 4.3
P(1-VAL-10)		0.16 ± 0.00	48.0 ± 7.7
P(1-VAL-12)		0.26 ± 0.02	50.0 ± 2.6

4.3. *Higuchi Model Fitting for Etoricoxib Release from PEU Films.*

Release results were fit to a kinetic model to quantitatively understand the mechanism behind which etoricoxib is releasing from the films and to predict how long it would take for full release of drug. The Higuchi model was determined to best fit the results as it intended for thin films. The model assumes (i) total sink condition at all times, (ii) release from only one-dimension, (iii) initial drug concentration in the film is much higher

than the drug solubility, (iv) drug particles are much smaller than the film thickness, (v) swelling and dissolution of the film are negligible, and (vi) the diffusivity of the drug is constant.[95] These assumptions were considered to be maintained throughout the study.

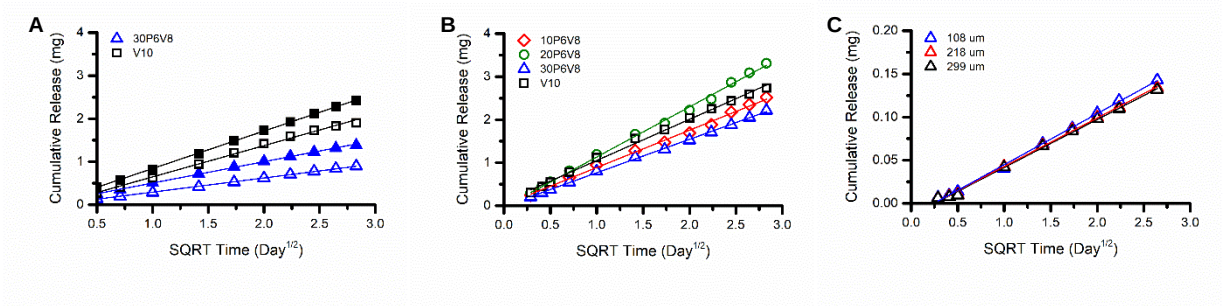

Figure 4.5. Higuchi model fitting for all tested films. The respective polymers are labeled with different colors and the 20% drug-loaded films are labelled with empty shapes while the 40% films are filled shapes. Variables analyzed for diffusivity were (A) drug-load, (B) polymer composition, and (C) thickness. Diffusivity constants were calculated using the linear fit equation and used to estimate the time for 100% of the drug to be released. All linear fits had a Pearson square value of 0.97 or above.

To fit the data, the cumulative release (mg) was plotted against the square root of time, as described (Figure 4.5). All plots remained linear for the entire time frame of data collection (R^2 =0.99). From these plots, the diffusivity constant was determined using the following equation:

$$D = \frac{(slope/A)^2}{2CC_s}$$

Where the slope is the amount of drug released at time t divided by the square root of time, A is the area of the film, C is the initial drug concentration (or the drug-load in the polymer), C_s is the drug solubility in the media (0.5 mg/mL) and D is the diffusivity constant. This constant not only indicates the mobility of the drug from the film into the media, but also can be used to calculate for the time of total release using the maximum amount of drug within the film (Table 4.10).

Table 4.10. Higuchi model data of all factors analyzed. Diffusivity was calculated using the Higuchi equation and time for total release of etoricoxib from the film was calculated by extrapolating the linear fit of the cumulative release (mg) versus the square root of time.

Polymer	Drug-load (%)	Thickness (μm)	Diffusivity Constant (cm^2/s)	$t_{100\%}$ (days)
10% 1-PHE-6 P(1-VAL-8)	20	87	5.79×10^{-6}	86
20% 1-PHE-6 P(1-VAL-8)	20	51	1.05×10^{-5}	21
30% 1-PHE-6 P(1-VAL-8)	20	44	4.68×10^{-6}	51
P(1-VAL-10)	20	38	7.10×10^{-6}	21
30% 1-PHE-6 P(1-VAL-8)	20	84	8.08×10^{-7}	36
30% 1-PHE-6 P(1-VAL-8)	40	83.5	8.46×10^{-6}	187
P(1-VAL-10)	20	85	3.01×10^{-6}	63
P(1-VAL-10)	40	100	2.81×10^{-6}	95
30% 1-PHE-6 P(1-VAL-8)	20	78	1.67×10^{-6}	49
30% 1-PHE-6 P(1-VAL-8)	20	200	1.57×10^{-6}	1636
30% 1-PHE-6 P(1-VAL-8)	20	430	1.42×10^{-6}	8577

Differences in total release time can be noted for both polymer composition, drug-load, and thickness with the most etoricoxib releasing from 20P6V8 and V10 at 20% drug-load, relative to all time points measured. This is more accurately suggested by the diffusivity constants, which can be compared relatively. The constants vary between all tested factors, suggesting that they impact how the etoricoxib is distributed in the film and therefore how it releases from the films. Total amount released, diffusivity constant, and the predicted time for total release all follow the same trend between all films tested; any and can be used to compare differences in release between samples. These results quantitatively correlate with the release results discussed above. Specifically, the higher drug loaded and thicker films were predicted to take longer to release 100% of the etoricoxib from the film, administering longer analgesia to the patient. Additionally, the diffusivity constants for the various polymer compositions describe the movement of etoricoxib out of the film in a similar manner that was described above. The phenylalanine

copolymer diffusivity constants suggest a slower release of etoricoxib that can be explained by the effects of intermolecular forces (e.g. pi-pi interactions). Moving forward, the Higuchi model can be used to accurately tune the matrix in a way to obtain a desired release profile and end point for dosage-specific applications.

4.4. *Multi-modal Analgesic Modeling.*

To quantitatively assess the diffusion of etoricoxib and bupivacaine out of the valine-based PEU films, Higuchi modeling was also used to fit the release data. Similar to the data shown above, all the Higuchi graphs reveal a linear trend with regression at 0.98 or above (Figure 4.6). As previously mentioned, the more hydrophobic the polymer chain, the higher the diffusivity constant an therefore the quicker the release (Table 4.11). Moreover, the time for total drug release also decreases with increasing diol chain length in the valine-based PEU films. This model not only gives us proof of concept that a multi-modal analgesia device is possible through these films, but also gives us an additional proof of the chemical or polymer composition effect on drug release rate and length.

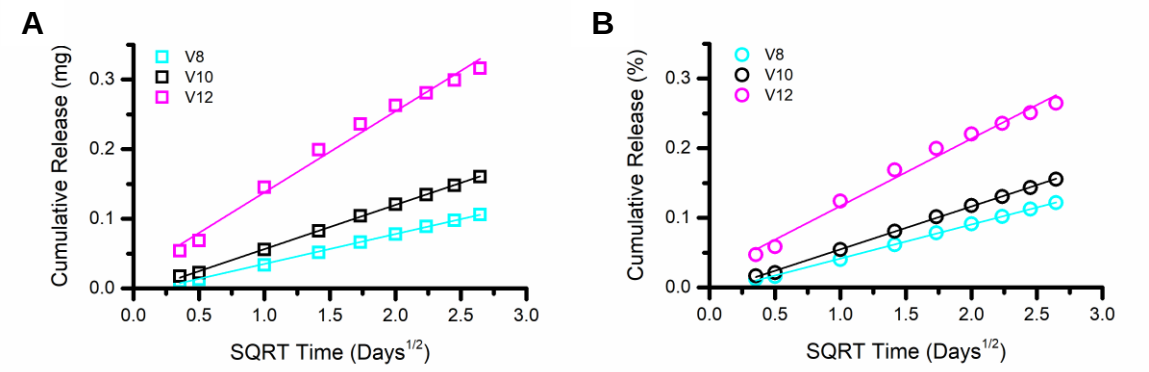

Figure 4.6. Higuchi fitting of bupivacaine and etoricoxib release from valine-based PEU films. Bupivacaine data is indicated by squares (A) and etoricoxib data is labeled with circles (B). Different colors represent different polymers (see graph legends).

Table 4.11. Higuchi model data of etoricoxib and bupivacaine valine-based PEU films. Diffusivity was calculated using the Higuchi equation and time for total release of etoricoxib from the film was calculated by extrapolating the linear fit of the cumulative release (mg) versus the square root of time.

Polymer	Drug	Thickness (μm)	Diffusivity Constant (cm^2/s)	$t_{100\%}$ (days)
P(1-VAL-8)	Bupivacaine	177	9.66×10^{-8}	85
P(1-VAL-10)		110	2.19×10^{-7}	25
P(1-VAL-12)		160	7.18×10^{-7}	21
P(1-VAL-8)	Etoricoxib	177	1.26×10^{-7}	110
P(1-VAL-10)		110	2.06×10^{-7}	30
P(1-VAL-12)		160	4.95×10^{-7}	28

4.5. *In Vivo Release.*

Plasma concentration was taken from the tail vein every fifteen minutes for 11 days to measure the amount of etoricoxib releasing from the films (μmol/L). This value was then used to determine the cumulative release of etoricoxib per time point (mg) (Figure 4.7). An initial burst was observed in the plasma concentration but following that etoricoxib release remained steady and continued through day 11.

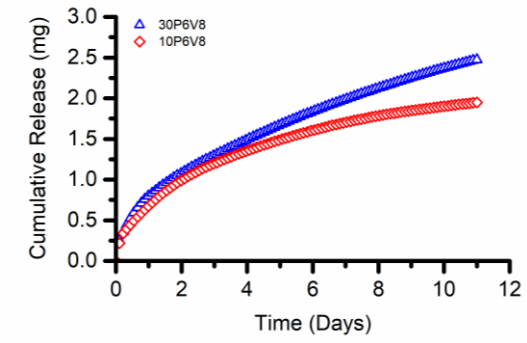

Polymer	Drug Release at Day 7 (mg)	Drug Release at Day 7 (%)
30% 1-PHE-6 P(1-VAL-8)	1.99 ± 0.34	22.1 ± 3.7
10% 1-PHE-6 P(1-VAL-8)	1.73 ± 0.49	19.2 ± 5.4

Figure 4.7. Cumulative release of implanted etoricoxib films as calculated from the plasma concentration *in vivo.* Two copolymer compositions were used, 10% and 30% 1-PHE-6 P(1-VAL-8). Values for cumulative release at day 7 are tabulated to the right for quantitative measure.

Once the study terminated, the degree of local delivery was obtained by excising the surrounding tissue of the film and determining the amount of etoricoxib it contained. This value was then compared to the amount of etoricoxib in the plasma at day 11. The average amount of etoricoxib in the local tissue was at least a 10-fold increase from the amount in the plasma (0.23 ± 0.05 mg to 0.01 ± 0.00 mg for 10P6V8 and 0.35 ± 0.08 mg to 0.02 ± 0.01 mg for 30P6V8). This suggests that local delivery was maintained. Moreover, further supporting this theory, the animals displayed signs of comfort and no inflammatory response was observed following the end of the study. Overall, films were incorporated well *in vivo* and provided local analgesia to the animal for the duration of the study. For quicker release, different polymer composition will be tried for future work as well as be implemented into different animal models to determine longer term effects of the films.

CHAPTER V

SUMMARY

Postoperative pain management remains a challenge following major surgery. With the over prescription of opioid pain management drugs, alternative strategies to manage pain must be employed. Herein, a series of poly(ester urea) homopolymers and copolymers were synthesized, mixed with etoricoxib, and fabricated in to local drug delivery films. The recommended dose of etoricoxib for a human is anywhere from 30-120 mg daily, depending on the patient and the severity of pain.[97,98] In a rat model, the appropriate dose scale for etoricoxib was determined by Merck to be 9 mg. By changing various factors of fabrication for PEU films, the tunable, controlled release of a model analgesic compound has been exhibited in this work.

By tuning film thickness, drug load, and/or polymer composition, the diffusion of drug out of the matrix can be selectively controlled to achieve the appropriate amount of analgesia needed. By understanding how each factor impacts the diffusion of etoricoxib out of the film, release can be slowed or accelerated. A quantitative measure of this was also obtained by fitting the release data to the Higuchi model for thin films. In a rat model, the films produced a therapeutic sensation as determined by the pain model used, suggesting effective and efficacious delivery of the analgesic compound. After 11 days, using the 10P6V8 and 30P6V8 copolymers, about 3 mg of etoricoxib was delivered to the

animal, with evidence of local delivery to the surrounding tissue before being metabolized into the bloodstream. However, a faster drug release is desired for pain management. In order to achieve this, the various factors studied in this work can be used to hasten the release.

In summary, this work displayed the benefits of drug-loaded PEU films that are able to achieve different release profiles implemented by fabrication controls. It was suggested that intermolecular forces play a significant role in the release of drug from PEU films. Mainly, both π-π interactions and hydrogen bonding impact how the drugs are able to diffuse out of the matrix. A better measure of the degree of both these forces would greatly benefit the understanding of how drug are behaving in these systems and will be done in future work.[99] Having control over release is useful for considering individualized treatment for pain post-operatively. For the future, valine-based PEUs will be tried *in vivo* to achieve quicker drug release with both etoricoxib and combination films. Overall, this work exemplified the potential of PEU films for post-operative pain management for the replacement or to limit the need for prescription opioids.

REFERENCES

(1) Kehlet, H.; Dahl, J. B. Anaesthesia, Surgery, and Challenges in Postoperative Recovery. *Lancet* **2003**, *362* (9399), 1921–1928.

(2) Weiser, T. G.; Regenbogen, S. E.; Thompson, K. D.; Haynes, A. B.; Lipsitz, S. R.; Berry, W. R.; Gawande, A. A. An Estimation of the Global Volume of Surgery: A Modelling Strategy Based on Available Data. *Lancet* **2008**, *372* (9633), 139–144.

(3) Gan, T. J.; Habib, A. S.; Miller, T. E.; White, W.; Apfelbaum, J. L. Incidence, Patient Satisfaction, and Perceptions of Post-Surgical Pain: Results from a US National Survey. *Curr. Med. Res. Opin.* **2014**, *30* (1), 149–160.

(4) Vadivelu, N.; Mitra, S.; Narayan, D. Recent Advances in Postoperative Pain Management. *Yale J. Biol. Med.* **2010**, *83* (1), 11–25.

(5) Alam, A. Long-Term Analgesic Use After Low-Risk Surgery. *Arch. Intern. Med.* **2012**.

(6) Clarke, H.; Soneji, N.; Ko, D. T.; Yun, L.; Wijeysundera, D. N. Rates and Risk Factors for Prolonged Opioid Use after Major Surgery: Population Based Cohort Study. *BMJ* **2014**, *349*, 1251–1241.

(7) Brummett, C. M.; Waljee, J. F.; Goesling, J.; Moser, S.; Lin, P.; Englesbe, M. J.; Bohnert, A. S. B.; Kheterpal, S.; Nallamothu, B. K. New Persistent Opioid Use after Minor and Major Surgical Procedures in Us Adults. *JAMA Surg.* **2017**, *152* (6), e170504.

(8) Soneji, N.; Clarke, H. A.; Ko, D. T.; Wijeysundera, D. N. Risks of Developing Persistent Opioid Use after Major Surgery. *JAMA Surg.* **2016**, *151* (11), 1083–1084.

(9) Tellegen, A. R.; Rudnik-Jansen, I.; Beukers, M.; Miranda-Bedate, A.; Bach, F. C.; de Jong, W.; Woike, N.; Mihov, G.; Thies, J. C.; Meij, B. P.; et al. Intradiscal Delivery of Celecoxib-Loaded Microspheres Restores Intervertebral Disc Integrity in a Preclinical Canine Model. *J. Control. Release* **2018**, *286*, 439–450.

(10) Wilsey, J. T.; Block, J. H. Sustained Analgesic Effect of Clonidine Co-Polymer Depot in a Porcine Incisional Pain Model. *J. Pain Res.* **2018**, *11*, 693–701.

(11) Kovaliov, M.; Li, S.; Korkmaz, E.; Cohen-Karni, D.; Tomycz, N.; Ozdoganlar, O. B.; Averick, S. Extended-Release of Opioids Using Fentanyl-Based Polymeric Nanoparticles for Enhanced Pain Management. *RSC Adv.* **2017**, *7*, 47904–47912.

(12) Pek, Y. S.; Pitukmanorom, P.; Ying, J. Y. Sustained Release of Bupivacaine for Post-Surgical Pain Relief Using Core-Shell Microspheres. *J. Mater. Chem. B* **2014**.

(13) Shepherd, S. D.; O'Buckley, S. C.; Harrington, J. M.; Haines, L. G.; Rothrock, G. D.; Johnson, L. M.; Nackley, A. G. A Moldable Sustained Release Bupivacaine Formulation for Tailored Treatment of Postoperative Dental Pain. *Sci. Rep.* **2018**, *8* (1), 12172.

(14) Tseng, Y. Y.; Liu, S. J. Nanofibers Used for the Delivery of Analgesics. *Nanomedicine* **2015**, *10* (11), 1786–1800.
(15) Research, G. V. *Biomaterials Market Size, Share & Trends Analysis Report By Product (Natural, Metallic, Ceramics, Polymers), By Application (Cardiovascular, Orthopedics, Plastic Surgery), And Segment Forecasts, 2018 - 2025*; 2018.
(16) Sáenz, A.; Rivera-muñoz, E.; Brostow, W.; Castaño, V. M.; Física, E. De; Rica, U. D. C.; Jose, S.; Rica, C.; Ciencias, F. De; Ingeniería, Q.; et al. Ceramic Biomaterials: An Introductory Overview. *J. Mater. Educ.* **1999**, *21* (5–6), 297–306.
(17) Kohane, D. S.; Langer, R. Polymeric Biomaterials in Tissue Engineering. *Pediatr. Res.* **2008**, *63*, 487–491.
(18) Niechajev, I. Facial Reconstruction Using Porous High-Density Polyethylene (Medpor): Long-Term Results. *Aesthetic Plast. Surg.* **2012**, *36* (4), 917–927.
(19) Hunter, A. C.; Moghimi, S. M. Smart Polymers in Drug Delivery: A Biological Perspective. *Polym. Chem.* **2017**, *8*, 41–51.
(20) Stewart, S. A.; Domínguez-Robles, J.; Donnelly, R. F.; Larrañeta, E. Implantable Polymeric Drug Delivery Devices: Classification, Manufacture, Materials, and Clinical Applications. *Polymers (Basel).* **2018**, *10* (12), 1–24.
(21) Teo, A. J. T.; Mishra, A.; Park, I.; Kim, Y.-J.; Park, W.-T.; Yoon, Y.-J. Polymeric Biomaterials for Medical Implants and Devices. *ACS Biomater. Sci. Eng.* **2016**, *2* (4), 454–472.
(22) Fu, K.; Pack, D. W.; Klibanov, A. M.; Langer, R. Visual Evidence of Acidic Environment within Degrading Poly(Lactic-Co- Glycolic Acid) (PLGA) Microspheres. *Pharm. Res.* **2000**, *17* (1), 100–106.
(23) Langer, R. Polymer Implants for Drug Delivery in the Brain. *J. Control. Release* **1991**, *16* (1–2), 53–59.
(24) Rosen, H. B.; Chang, J.; Wnek, G. E.; Linhardt, R. J.; Langer, R. Bioerodible Polyanhydrides for Controlled Drug Delivery. *Biomaterials* **1983**, *4* (2), 131–133.
(25) Leong, K. W.; Kost, J.; Mathiowitz, E.; Langer, R. Polyanhydrides for Controlled Release of Bioactive Agents. *Biomaterials* **1986**, *7* (5), 364–371.
(26) Tam, J.; Anger, R. L. The Development of Polyanhydrides for Drug Delivery Applications. *J. Biomater. Sci. Polym. Ed.* **1992**, *3* (4), 315–353.
(27) Vogel, B. M.; Mallapragada, S. K. Synthesis of Novel Biodegradable Polyanhydrides Containing Aromatic and Glycol Functionality for Tailoring of Hydrophilicity in Controlled Drug Delivery Devices. *Biomaterials* **2005**, *26* (7), 721–728.
(28) Kipper, M. J.; Shen, E.; Determan, A.; Narasimhan, B. Design of an Injectable System Based on Bioerodible Polyanhydride Microspheres for Sustained Drug Delivery. *Biomaterials* **2002**, *23* (22), 4405–4412.
(29) Sharpe, L. A.; Vela Ramirez, J. E.; Haddadin, O. M.; Ross, K. A.; Narasimhan, B.; Peppas, N. A. PH-Responsive Microencapsulation Systems for the Oral Delivery of Polyanhydride Nanoparticles. *Biomacromolecules* **2018**, *19* (3), 793–802.
(30) Torres, M. P.; Determan, A. S.; Anderson, G. L.; Mallapragada, S. K.; Narasimhan, B. Amphiphilic Polyanhydrides for Protein Stabilization and Release. *Biomaterials* **2007**, *28* (1), 108–116.
(31) Liu, X.; Pettway, G. J.; McCauley, L. K.; Ma, P. X. Pulsatile Release of

Parathyroid Hormone from an Implantable Delivery System. *Biomaterials* **2007**, *28* (28), 4124–4131.
(32) Dang, M.; Koh, A. J.; Jin, X.; McCauley, L. K.; Ma, P. X. Local Pulsatile PTH Delivery Regenerates Bone Defects via Enhanced Bone Remodeling in a Cell-Free Scaffold. *Biomaterials* **2017**, *114*, 1–9.
(33) Wang, P. P.; Frazier, J.; Brem, H. Local Drug Delivery to the Brain. *Adv. Drug Deliv. Rev.* **2002**, *54* (7), 987–1013.
(34) Berrada, M.; Yang, Z.; Lehnert, S. Tumor Treatment by Sustained Intratumoral Release of 5-Fluorouracil: Effects of Drug Alone and in Combined Treatments. *Int. J. Radiat. Oncol. Biol. Phys.* **2002**, *54* (5), 1550–1557.
(35) Storm, P. B.; Moriarity, J. L.; Tyler, B.; Burger, P. C.; Brem, H.; Weingart, J. Polymer Delivery of Camptothecin against 9L Gliosarcoma: Release, Distribution, and Efficacy. *J. Neurooncol.* **2002**, *56* (3), 209–217.
(36) Wang, J.; Yang, G.; Guo, X.; Tang, Z.; Zhong, Z.; Zhou, S. Redox-Responsive Polyanhydride Micelles for Cancer Therapy. *Biomaterials* **2014**, *35* (9), 3080–3090.
(37) Sipos, E. P.; Tyler, B.; Piantadosi, S.; Burger, P. C.; Brem, H. Optimizing Interstitial Delivery of BCNU from Controlled Release Polymers for the Treatment of Brain Tumors. *Cancer Chemother. Pharmacol.* **1997**.
(38) Stephens, D.; Li, L.; Robinson, D.; Chen, S.; Chang, H. C.; Liu, R. M.; Tian, Y.; Ginsburg, E. J.; Gao, X.; Stultz, T. Investigation of the in Vitro Release of Gentamicin from a Polyanhydride Matrix. *J. Control. Release* **2000**, *63* (3), 305–317.
(39) Chiu Li, L.; Deng, J.; Stephens, D. Polyanhydride Implant for Antibiotic Delivery - From the Bench to the Clinic. *Adv. Drug Deliv. Rev.* **2002**, *54* (7), 963–986.
(40) Heller, J. Development of Poly(Ortho Esters): A Historical Overview. *Biomaterials* **1990**, *11* (9), 659–665.
(41) Heller, J.; Penhale, D. W. H.; Helwing, R. F. Preparation of Poly(Ortho Esters) by the Reaction of Diketene Acetals and Polyols. *J. Polym. Sci. Polym. Lett. Ed.* **1980**, *18*, 619–624.
(42) Heller, J.; Barr, J. Poly(Ortho Esters) - From Concept to Reality. *Biomacromolecules* **2004**, *5* (5), 1625–1632.
(43) Ng, S. Y.; Shen, H. R.; Lopez, E.; Zherebin, Y.; Barr, J.; Schacht, E.; Heller, J. Development of a Poly(Ortho Ester) Prototype with a Latent Acid in the Polymer Backbone for 5-Fluorouracil Delivery. *J. Control. Release* **2000**, *65* (3), 367–374.
(44) Rothen-Weinhold, A.; Schwach-Abdellaoui, K.; Barr, J.; Ng, S. Y.; Shen, H. R.; Gurny, R.; Heller, J. Release of BSA from Poly(Ortho Ester) Extruded Thin Strands. *J. Control. Release* **2001**, *71* (1), 31–37.
(45) Barr, J.; Woodburn, K. W.; Ng, S. Y.; Shen, H. R.; Heller, J. Post Surgical Pain Management with Poly(Ortho Esters). *Adv. Drug Deliv. Rev.* **2002**, *54*, 1041–1048.
(46) Knop, K.; Hoogenboom, R.; Fischer, D.; Schubert, U. S. Poly(Ethylene Glycol) in Drug Delivery: Pros and Cons as Well as Potential Alternatives. *Angew. Chemie - Int. Ed.* **2010**, *49*, 6288–6308.
(47) Kolate, A.; Baradia, D.; Patil, S.; Vhora, I.; Kore, G.; Misra, A. PEG - A Versatile Conjugating Ligand for Drugs and Drug Delivery Systems. *J. Control. Release*

2014, *192*, 67–81.
(48) Laurencin, B. D. U. L. S. N. C. T. Biomedical Applications of Biodegradable Polymers. *J Polym Sci B Polym Phys. 2011 June 15; 49(12) 832–864.* **2011**, *49* (12), 832–864.
(49) Gou, M.; Wu, L.; Yin, Q.; Guo, Q.; Guo, G.; Liu, J.; Zhao, X.; Wei, Y.; Qian, Z. Transdermal Anaesthesia with Lidocaine Nano-Formulation Pretreated with Low-Frequency Ultrasound in Rats Model. *J. Nanosci. Nanotechnol.* **2009**, *9* (11), 6360–6365.
(50) Cohn, D.; Hotovely Salomon, A. Designing Biodegradable Multiblock PCL/PLA Thermoplastic Elastomers. *Biomaterials* **2005**, *26*, 2297–2305.
(51) Cutright, D. E.; Beasley, J. D.; Perez, B. Histologic Comparison of Polylactic and Polyglycolic Acid Sutures. *Oral Surgery, Oral Med. Oral Pathol.* **1971**, *32* (1), 165–173.
(52) Frazza, E. J.; Schmitt, E. E. A New Absorbable Suture. *J. Biomed. Mater. Res.* **1971**, *5* (2), 43–58.
(53) Wang, X.; Wenk, E.; Hu, X.; Castro, G. R.; Meinel, L.; Wang, X.; Li, C.; Merkle, H.; Kaplan, D. L. Silk Coatings on PLGA and Alginate Microspheres for Protein Delivery. *Biomaterials* **2007**, *28* (28), 4161–4169.
(54) Kim, H. K.; Chung, H. J.; Park, T. G. Biodegradable Polymeric Microspheres with "Open/Closed" Pores for Sustained Release of Human Growth Hormone. *J. Control. Release* **2006**, *112* (2), 167–174.
(55) Ungaro, F.; D'Angelo, I.; Coletta, C.; D'Emmanuele Di Villa Bianca, R.; Sorrentino, R.; Perfetto, B.; Tufano, M. A.; Miro, A.; La Rotonda, M. I.; Quaglia, F. Dry Powders Based on PLGA Nanoparticles for Pulmonary Delivery of Antibiotics: Modulation of Encapsulation Efficiency, Release Rate and Lung Deposition Pattern by Hydrophilic Polymers. *J. Control. Release* **2012**, *157* (1), 149–159.
(56) Toti, U. S.; Guru, B. R.; Hali, M.; McPharlin, C. M.; Wykes, S. M.; Panyam, J.; Whittum-Hudson, J. A. Targeted Delivery of Antibiotics to Intracellular Chlamydial Infections Using PLGA Nanoparticles. *Biomaterials* **2011**, *32* (27), 6606–6613.
(57) Shepherd, S. D.; O'Buckley, S. C.; Harrington, J. M.; Haines, L. G.; Rothrock, G. D.; Johnson, L. M.; Nackley, A. G. A Moldable Sustained Release Bupivacaine Formulation for Tailored Treatment of Postoperative Dental Pain. *Sci. Rep.* **2018**, *8* (12172).
(58) Jain, R. A. The Manufacturing Techniques of Various Drug Loaded Biodegradable Poly(Lactide-Co-Glycolide) (PLGA) Devices. *Biomaterials* **2000**, *21*, 2475–2490.
(59) Ensign, L. M.; Tang, B. C.; Wang, Y. Y.; Tse, T. A.; Hoen, T.; Cone, R.; Hanes, J. Mucus-Penetrating Nanoparticles for Vaginal Drug Delivery Protect against Herpes Simplex Virus. *Sci. Transl. Med.* **2012**, *4* (138), 138ra179.
(60) Schneider, C. S.; Xu, Q.; Boylan, N. J.; Chisholm, J.; Tang, B. C.; Schuster, B. S.; Henning, A.; Ensign, L. M.; Lee, E.; Adstamongkonkul, P.; et al. Nanoparticles That Do Not Adhere to Mucus Provide Uniform and Long-Lasting Drug Delivery to Airways Following Inhalation. *Sci. Adv.* **2017**, *3* (4), e1601556.
(61) Shendruk, T. N.; Elliott Donaghue, I.; Tuladhar, A.; Pakulska, M. M.; McLaughlin, C. K.; Shoichet, M. S.; Obermeyer, J. M. Encapsulation-Free

Controlled Release: Electrostatic Adsorption Eliminates the Need for Protein Encapsulation in PLGA Nanoparticles. *Sci. Adv.* **2016**, *2* (5), e1600519.
(62) Bazile, D. V.; Ropert, C.; Huve, P.; Verrecchia, T.; Mariard, M.; Frydman, A.; Veillard, M.; Spenlehauer, G. Body Distribution of Fully Biodegradable [14C]-Poly(Lactic Acid) Nanoparticles Coated with Albumin after Parenteral Administration to Rats. *Biomaterials* **1992**, *13* (15), 1093–1102.
(63) Tobío, M.; Gref, R.; Sánchez, A.; Langer, R.; Alonso, M. J. Stealth PLA-PEG Nanoparticles as Protein Carriers for Nasal Administration. *Pharm. Res.* **1998**, *15* (2), 270–275.
(64) Khodaverdi, E.; Hadizadeh, F.; Tekie, F. S. M.; Jalali, A.; Mohajeri, S. A.; Ganji, F. Preparation and Analysis of a Sustained Drug Delivery System by PLGA-PEG-PLGA Triblock Copolymers. *Polym. Bull.* **2012**, *69* (4), 429–438.
(65) Miyazaki, M.; Maeda, T.; Hirashima, K.; Kurokawa, N.; Nagahama, K.; Hotta, A. PEG-Based Nanocomposite Hydrogel: Thermoresponsive Sol-Gel Transition Controlled by PLGA-PEG-PLGA Molecular Weight and Solute Concentration. *Polymer (Guildf).* **2017**, *115*, 246–254.
(66) Wang, Z.; Huang, H.; Yang, S.; Huang, S.; Guo, J.; Tang, Q.; Qi, F. Long-Term Effect of Ropivacaine Nanoparticles for Sciatic Nerve Block on Postoperative Pain in Rats. *Int. J. Nanomedicine* **2016**, *11*, 2081–2090.
(67) Tobe, M.; Obata, H.; Suto, T.; Yokoo, H.; Nakazato, Y.; Tabata, Y.; Saito, S. Long-Term Effect of Sciatic Nerve Block with Slow-Release Lidocaine in a Rat Model of Postoperative Pain. *Anesthesiology* **2010**, *112* (6), 1473–1481.
(68) Liu, H.; Slamovich, E. B.; Webster, T. J. Less Harmful Acidic Degradation of Poly(Lactic-Co-Glycolic Acid) Bone Tissue Engineering Scaffolds through Titania Nanoparticle Addition. *Int. J. Nanomedicine* **2006**, *1* (4), 541–545.
(69) Dreger, N. Z.; Wandel, M. B.; Robinson, L. L.; Luong, D.; Søndergaard, C. S.; Hiles, M.; Premanandan, C.; Becker, M. L. Preclinical in Vitro and in Vivo Assessment of Linear and Branched l -Valine-Based Poly(Ester Urea)s for Soft Tissue Applications. *ACS Biomater. Sci. Eng.* **2018**, *4* (4), 1346–1356.
(70) Yu, J.; Lin, F.; Lin, P.; Gao, Y.; Becker, M. L. Phenylalanine-Based Poly(Ester Urea): Synthesis, Characterization, and in Vitro Degradation. *Macromolecules* **2014**, *47* (1), 121–129.
(71) Gao, Y.; Childers, E. P.; Becker, M. L. L -Leucine-Based Poly(Ester Urea)s for Vascular Tissue Engineering. *ACS Biomater. Sci. Eng.* **2015**, *1* (9), 795–804.
(72) Apfelbaum, J. L.; Chen, C.; Mehta, S. S.; Gan, T. J. Postoperative Pain Experience: Results from a National Survey Suggest Postoperative Pain Continues to Be Undermanaged. *Anesth. Analg.* **2003**, *97* (2), 534–540.
(73) Wunsch, H.; Wijeysundera, D. N.; Passarella, M. A.; Neuman, M. D. Opioids Prescribed after Low-Risk Surgical Procedures in the United States, 2004-2012. *JAMA - J. Am. Med. Assoc.* **2016**, *125* (5), 1733–1740.
(74) Bicket, M. C.; Long, J. J.; Pronovost, P. J.; Alexander, G. C.; Wu, C. L. Prescription Opioid Analgesics Commonly Unused after Surgery: A Systematic Review. *JAMA Surg.* **2017**, *152* (11), 1066–1071.
(75) Hughes, A.; Williams, M. R.; Lipari, R. N.; Bose, J.; Copello, E. A. P.; Kroutil, L. A. Prescription Drug Use and Misuse in the United States: Results from the 2015 National Survey on Drug Use and Health. *NSDUH Data Review*. 2016.

(76) Stein, C.; Lang, L. J. Peripheral Mechanisms of Opioid Analgesia. *Curr. Opin. Pharmacol.* **2009**, *76* (1), 182–191.
(77) Millan, M. J. Multiple Opioid Systems and Pain. *Pain* **1986**, *27* (3), 303–347.
(78) Vaughan, C. W.; Ingram, S. L.; Connor, M. A.; Christie, M. J. How Opioids Inhibit GABA-Mediated Neurotransmission. *Nature* **1997**, *390*, 611–614.
(79) Manworren, R. C. B. Multimodal Pain Management and the Future of a Personalized Medicine Approach to Pain. *AORN J.* **2015**, *101* (3), 307–319.
(80) Wick, E. C.; Grant, M. C.; Wu, C. L. Postoperativemultimodal Analgesia Pain Management with Nonopioid Analgesics and Techniques a Review. *JAMA Surg.* **2017**, *152* (7), 691–697.
(81) Lunn, T. H.; Husted, H.; Laursen, M. B.; Hansen, L. T.; Kehlet, H. Analgesic and Sedative Effects of Perioperative Gabapentin in Total Knee Arthroplasty: A Randomized, Double-Blind, Placebo-Controlled Dose-Finding Study. *Pain* **2015**, *156* (12), 2438–2448.
(82) Portenoy, R. K.; Sciberras, A.; Eliot, L.; Loewen, G.; Butler, J.; Devane, J. Steady-State Pharmacokinetic Comparison of a New, Extended-Release, Once-Daily Morphine Formulation, Avinza™, and a Twice-Daily Controlled-Release Morphine Formulation in Patients with Chronic Moderate-to-Severe Pain. *J. Pain Symptom Manage.* **2002**, *23* (4), 292–300.
(83) Candiotti, K. Liposomal Bupivacaine: An Innovative Nonopioid Local Analgesic for the Management of Postsurgical Pain. *Pharmacotherapy* **2012**, *32* (9), 19–26.
(84) Gambling, D.; Hughes, T.; Martin, G.; Horton, W.; Manvelian, G. A Comparison of Depodur™, a Novel, Single-Dose Extended-Release Epidural Morphine, with Standard Epidural Morphine for Pain Relief after Lower Abdominal Surgery. *Anesth. Analg.* **2005**, *100* (4), 1065–1074.
(85) Margetts, L.; Sawyer, R. Transdermal Drug Delivery: Principles and Opioid Therapy. *Contin. Educ. Anaesthesia, Crit. Care Pain* **2007**, *7* (5), 171–176.
(86) Oliashirazi, A.; Wilson-Byrne, T.; Shuler, F. D.; Parvizi, J. Patient-Controlled Fentanyl Iontophoretic Transdermal System Improved Postoperative Mobility Compared to Intravenous Patient-Controlled Analgesia Morphine: A Pooled Analysis of Randomized, Controlled Trials. *Pain Pract.* **2017**, *17* (2), 197–207.
(87) Larrañeta, E.; Lutton, R. E. M.; Woolfson, A. D.; Donnelly, R. F. Microneedle Arrays as Transdermal and Intradermal Drug Delivery Systems: Materials Science, Manufacture and Commercial Development. *Mater. Sci. Eng. R Reports* **2016**, *104*, 1–32.
(88) Hoy, S. M.; Keating, G. M. Fentanyl Transdermal Matrix Patch (Durotep® MT Patch; Durogesic® DTrans®; Durogesic® SMAT): In Adults with Cancer-Related Pain. *Drugs* **2008**, *68* (12), 1711–1721.
(89) Dankiewicz, E. H. Use of the Low-Dose Buprenorphine Patch: A Response. *J. Palliat. Med.* **2014**, *17* (4), 379–380.
(90) Dreger, N. Z.; Fan, Z.; Zander, Z. K.; Tantisuwanno, C.; Haines, M. C.; Waggoner, M.; Parsell, T.; Søndergaard, C. S.; Hiles, M.; Premanandan, C.; et al. Amino Acid-Based Poly(Ester Urea) Copolymer Films for Hernia-Repair Applications. *Biomaterials* **2018**, *182* (August), 44–57.
(91) Siepmann, J.; Peppas, N. A. Higuchi Equation: Derivation, Applications, Use and Misuse. *Int. J. Pharm.* **2011**, *418* (1), 6–12.

(92) Peterson, G. I.; Dobrynin, A. V.; Becker, M. L. α-Amino Acid-Based Poly(Ester Urea)s as Multishape Memory Polymers for Biomedical Applications. *ACS Macro Lett.* **2016**, *5* (10), 1176–1179.
(93) Ma, D.; McHugh, A. J. The Interplay of Membrane Formation and Drug Release in Solution-Cast Films of Polylactide Polymers. *Int. J. Pharm.* **2010**, *388* (1–2), 1–12.
(94) Dorta, J. M.; Oliva, A.; Munguia, O.; Llabres, M.; Farina, J. B. In-Vitro Release of Fluoropyrimidines from PLGA Film Implants. *J. Pharm. Pharmacol.* **2002**, *54* (6), 757–763.
(95) Higuchi, T. Mechanism of Sustained- Action Medication. *J. Pharm. Sci.* **1963**, *52*, 1145–1149.
(96) Chen, K.; Yu, J.; Guzman, G.; Es-Haghi, S. S.; Becker, M. L.; Cakmak, M. Role of Hydrogen Bonding on Nonlinear Mechano-Optical Behavior of l-Phenylalanine-Based Poly(Ester Urea)S. *Macromolecules* **2017**, *50* (3), 1075–1084.
(97) Escudero-Contreras, A.; Cervantes, J. V. M.; Collantes-Estevez, E. Update on the Clinical Pharmacology of Etoricoxib, a Potent Cyclooxygenase-2 Inhibitor. *Fut. Rheumatol.* **2007**, *2* (6), 545–565.
(98) Birmingham, B.; Buvanendran, A. Nonsteroidal Anti-Inflammatory Drugs, Acetaminophen, and COX-2 Inhibitors. In *Practical Management of Pain: Fifth Edition*; 2013; pp 553–568.
(99) Zhuang, W. R.; Wang, Y.; Cui, P. F.; Xing, L.; Lee, J.; Kim, D.; Jiang, H. L.; Oh, Y. K. Applications of π-π Stacking Interactions in the Design of Drug-Delivery Systems. *J. Control. Release* **2019**, *294*, 311–326.

APPENDICES

APPENDIX A. [1]HNMR of monomers: M(1-VAL-8), M(1-VAL-10), and M(1-PHE-6).

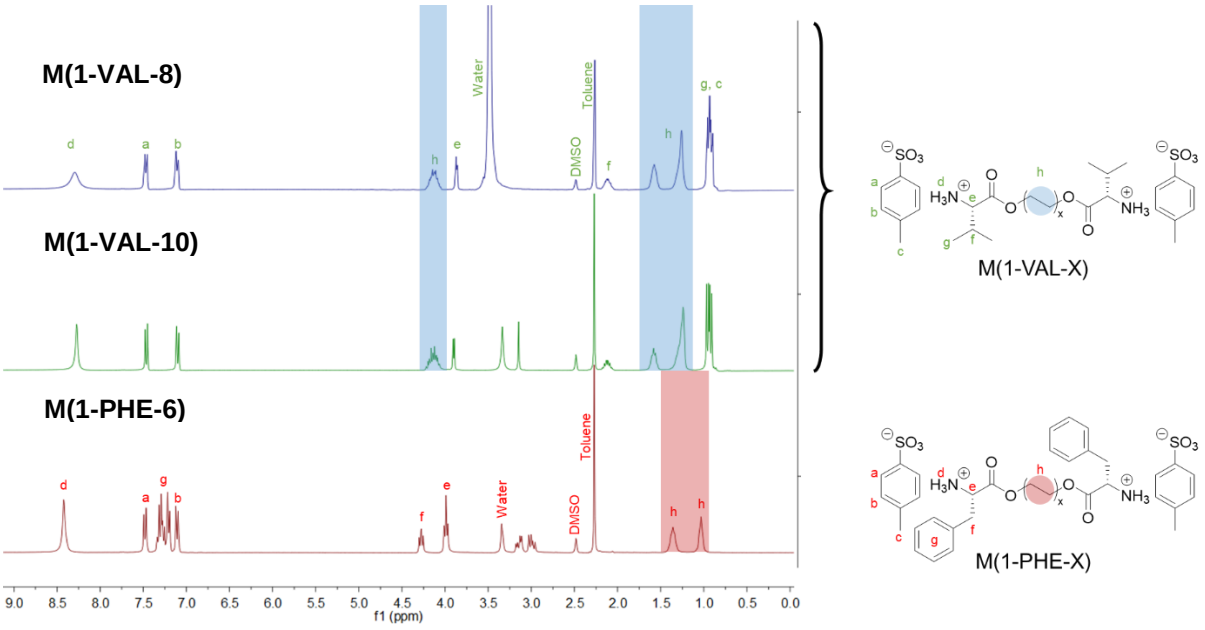

APPENDIX B. [1]HNMR of poly(ester urea) homopolymer and copolymers.

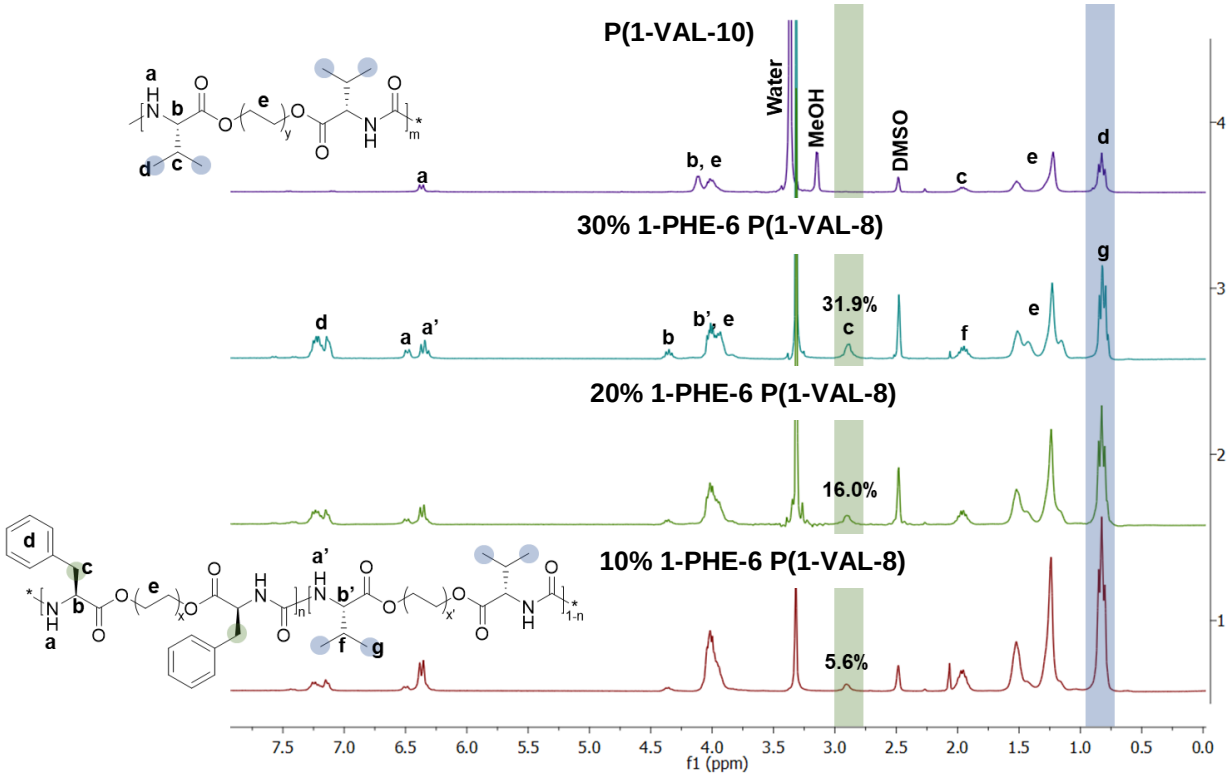

APPENDIX C. Characterization data of polymers.

Polymer	M_w (kDa)	M_n (kDa)	$Đ_m$	T_g (°C)	T_d (°C)
10% 1-PHE-6 P(1-VAL-8)	107	68	1.6	44	245
20% 1-PHE-6 P(1-VAL-8)	88	56	1.6	57	278
30% 1-PHE-6 P(1-VAL-8)	104	52	2.0	45	263
P(1-VAL-10)	216	143	1.5	42	275